Supporting Information

Multistage Antiplasmodium Activity of Astemizole Analogues and Inhibition of Hemozoin Formation as a Contributor to Their Mode of Action

Malkeet Kumar[1], John Okombo[1], Dickson Mambwe[1], Dale Taylor[2], Nina Lawrence[2], Janette Reader[3], Mariëtte van der Watt[3], Diana Fontinha[4], Margarida Sanches-Vaz[4], Belinda C Bezuidenhout[5], Sonja B Lauterbach[5], Dale Liebenberg[5], Lyn-Marie Birkholtz[3], Theresa L Coetzer[5], Miguel Prudêncio[4], Timothy J. Egan[1,6], Sergio Wittlin[7,8], Kelly Chibale[1,6,9]*

[1]Department of Chemistry, University of Cape Town, Rondebosch 7701, South Africa.

[2]Drug Discovery and Development Centre (H3D), Division of Clinical Pharmacology, Department of Medicine, University of Cape Town, Observatory 7925, South Africa.

[3]Department of Biochemistry, Genetics and Microbiology, Institute for Sustainable Malaria Control, University of Pretoria, Private Bag X20, Hatfield 0028, South Africa.

[4]Instituto de Medicina Molecular, Faculdade de Medicina, Universidade de Lisboa, Av. Prof. Egas Moniz, 1649-028 Lisboa, Portugal.

[5]Department of Molecular Medicine and Haematology, School of Pathology, Faculty of Health Sciences, University of the Witwatersrand and National Health Laboratory Service, Johannesburg 2193, South Africa

[6]Institute of Infectious Disease and Molecular Medicine, University of Cape Town, Rondebosch 7701, South Africa.

[7]Swiss Tropical and Public Health Institute, Socinstrasse 57, 4002 Basel, Switzerland

[8]University of Basel, 4003 Basel, Switzerland.

[9]South African Medical Research Council Drug Discovery and Development Research Unit, Department of Chemistry University of Cape Town, Rondebosch 7701, South Africa.

Table of contents

Supplementary Table S1: Melting points, solubility and β-haematin inhibitory activity (βHIA) values for AST, it metabolites and analogues tested in this study.

Compound Code	Melting Point (°C)	Kinetic Solubility (μM)	βHIA IC_{50} (μM)	[a]cLogP	[a]pKa	[b]hERG pC50
AST	169-171.5	90	130.5	5.84	9.19	8.26
DM-AST	180.5-182.3	200	55.2	5.25	9.19	8.17
Nor-AST	167.5-169	150	856.2	3.38	9.45	6.73
3	138-140.3	35	2000.0	5.83	8.0	7.98
5c	70-72	90	253.4	4.11	9.18	6.61
5d	138-140	155	2709.5	4.18	9.21	7.24
7	37-40	25	132.9	5.84	9.19	8.10
8	138-141	35	201.6	5.84	9.19	8.12
9	148-151	10	160.0	5.13	9.19	7.97
10	159-162	10	93.8	5.13	9.19	7.30
11	131-134	<5	97.5	5.13	9.19	7.82
12	126-129	20	964.8	5.51	9.19	6.54
13	182-184	20	3049.0	4.21	9.19	7.26
14	118-121	60	2640.0	4.05	9.19	7.88
15	146-148	5	65.2	5.13	9.19	8.07
16	200-202	30	3646.0	4.20	9.19	7.56
17	165-167	85.2	125.4	4.54	9.19	7.90

18	59-62	30	252.8	5.84	9.19	8.11
19	115-117	100	181.1	5.84	9.19	8.05
20	64-66	65	294.8	5.75	9.19	8.12
Hydrocortisone		195	-			
Reserpine		<5	-			
Chloroquine			23	5.06	10.01	6.21
Amodiaquine			11			
Halofantrine						7.36

[a]Calculate using ChemDraw Professional; [b]hERG pIC50: was determined using starDrop™ predictive software;

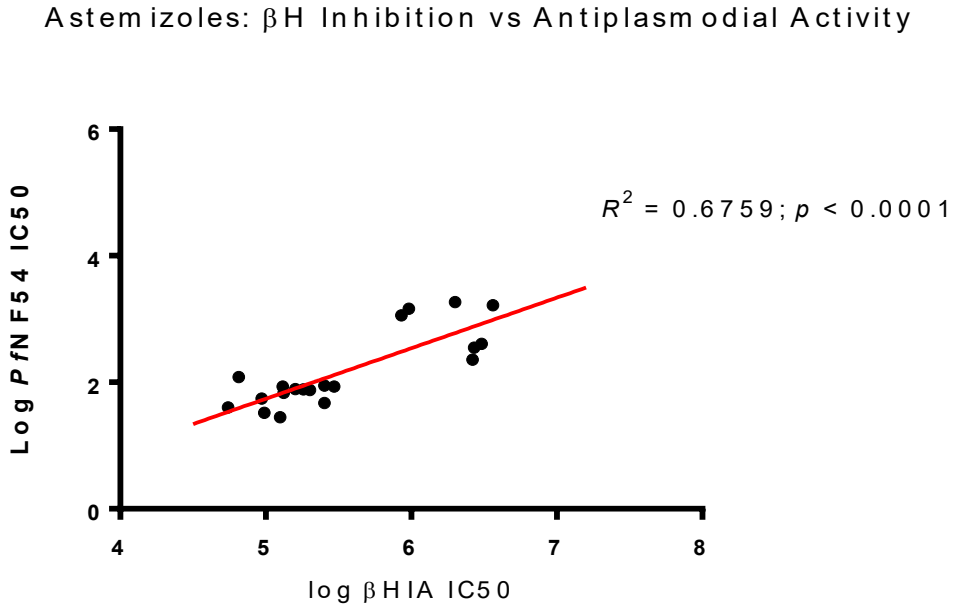

Figure S1: Linear correlation between βH inhibition and parasite growth IC_{50} values for *Pf*NF54. Measurements of βH and parasite growth inhibitions were both done in triplicates.

NMR spectra of astemizole analogues

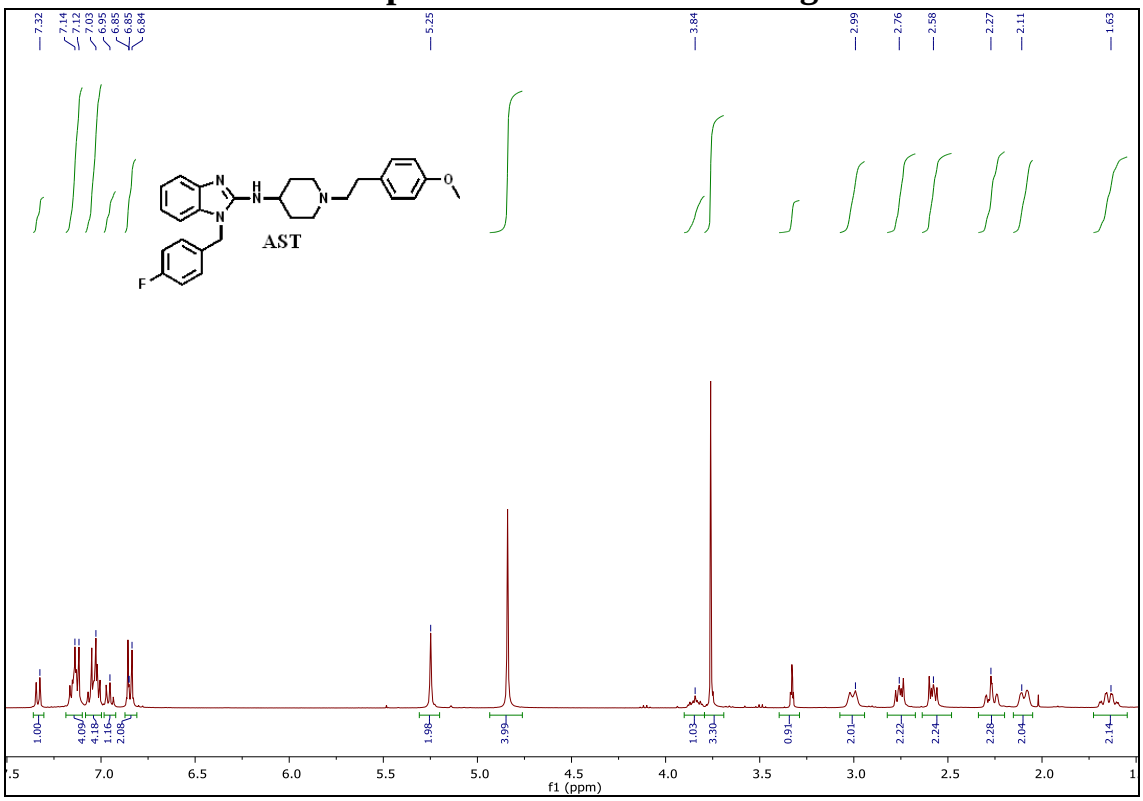

Figure S2: ^{1}H-NMR spectrum of AST in CD_3OD at 400 MHz.

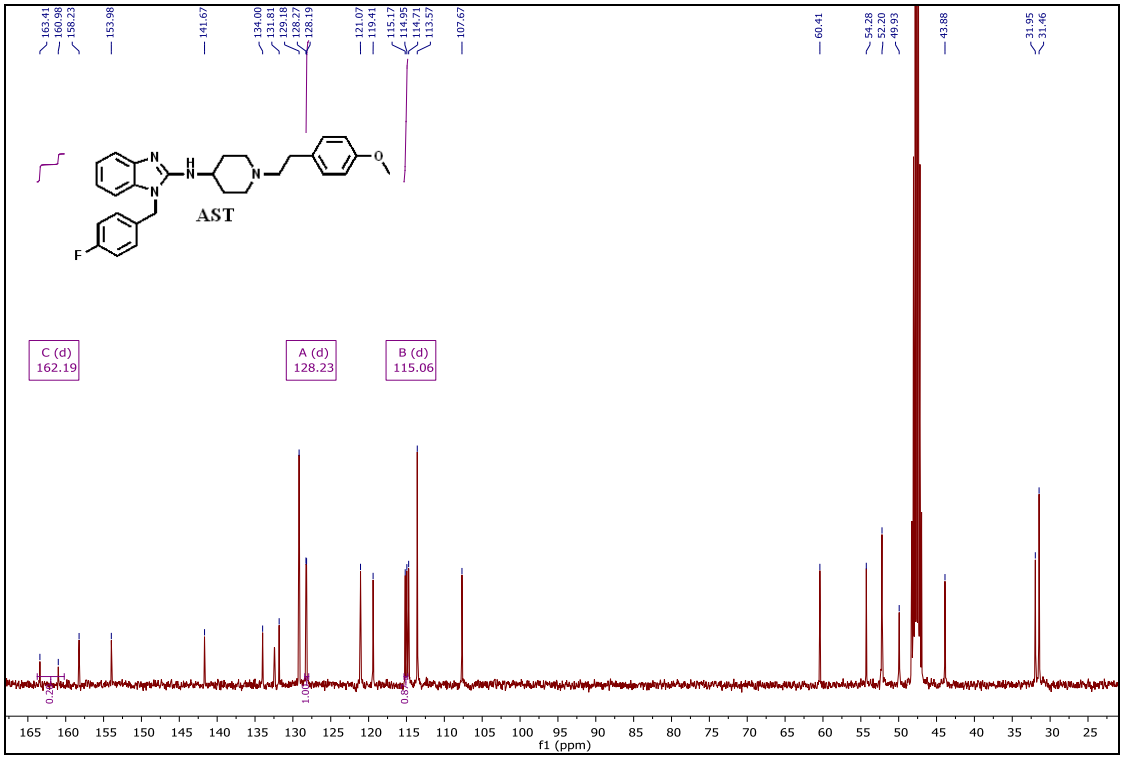

Figure S3: ^{13}C-NMR spectrum of AST in CD_3OD at 101 MHz.

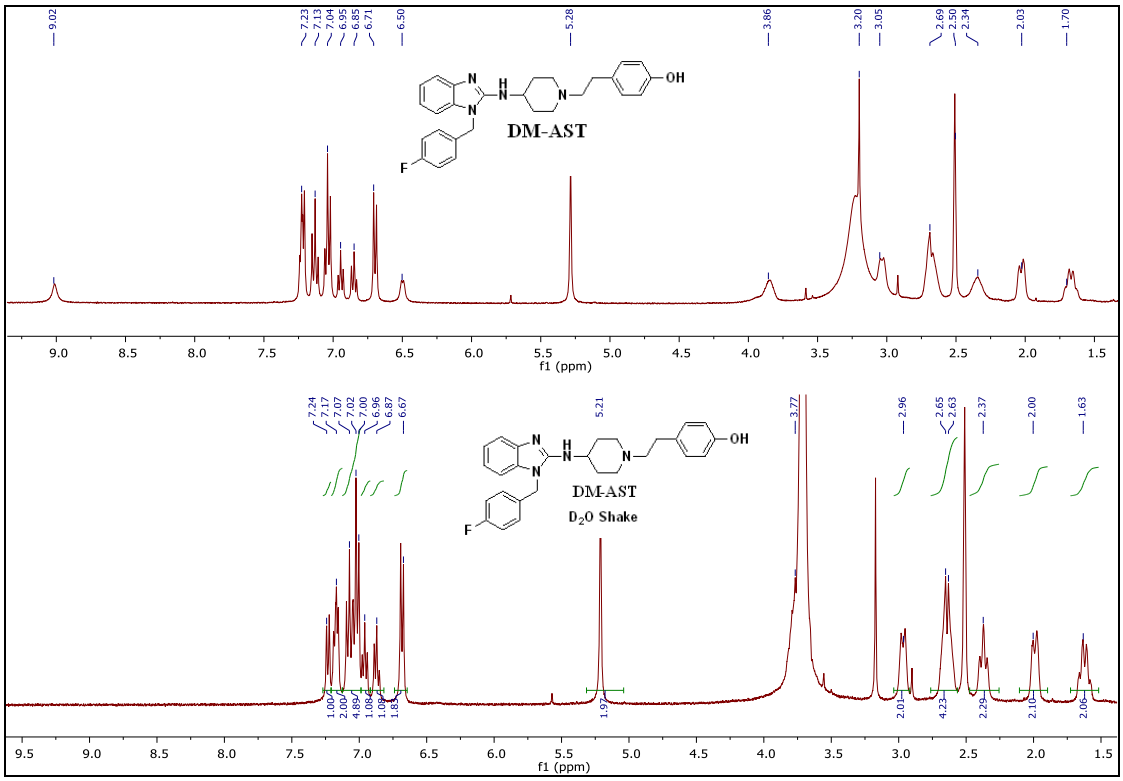

Figure S4: ^{1}H-NMR spectrum of DM-AST in CD_3OD at 400 MHz and D_2O shake experiment.

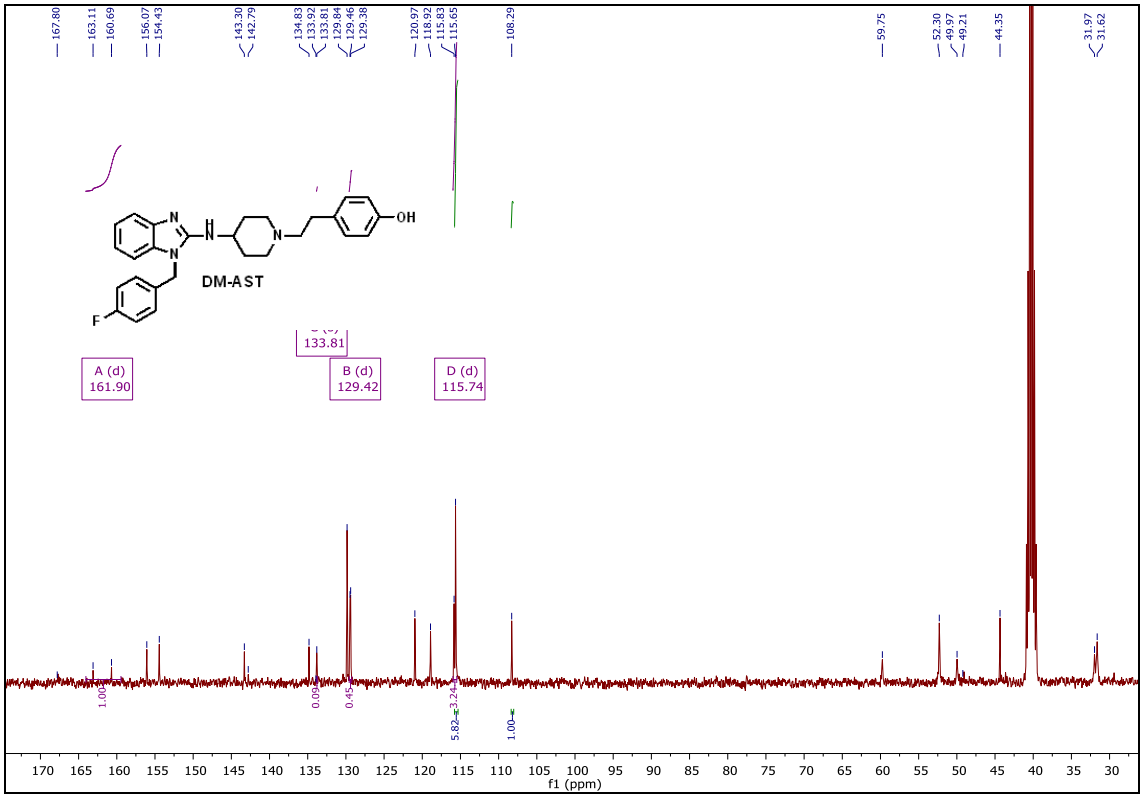

Figure S5: ^{13}C-NMR spectrum of DM-AST in CD_3OD at 101 MHz.

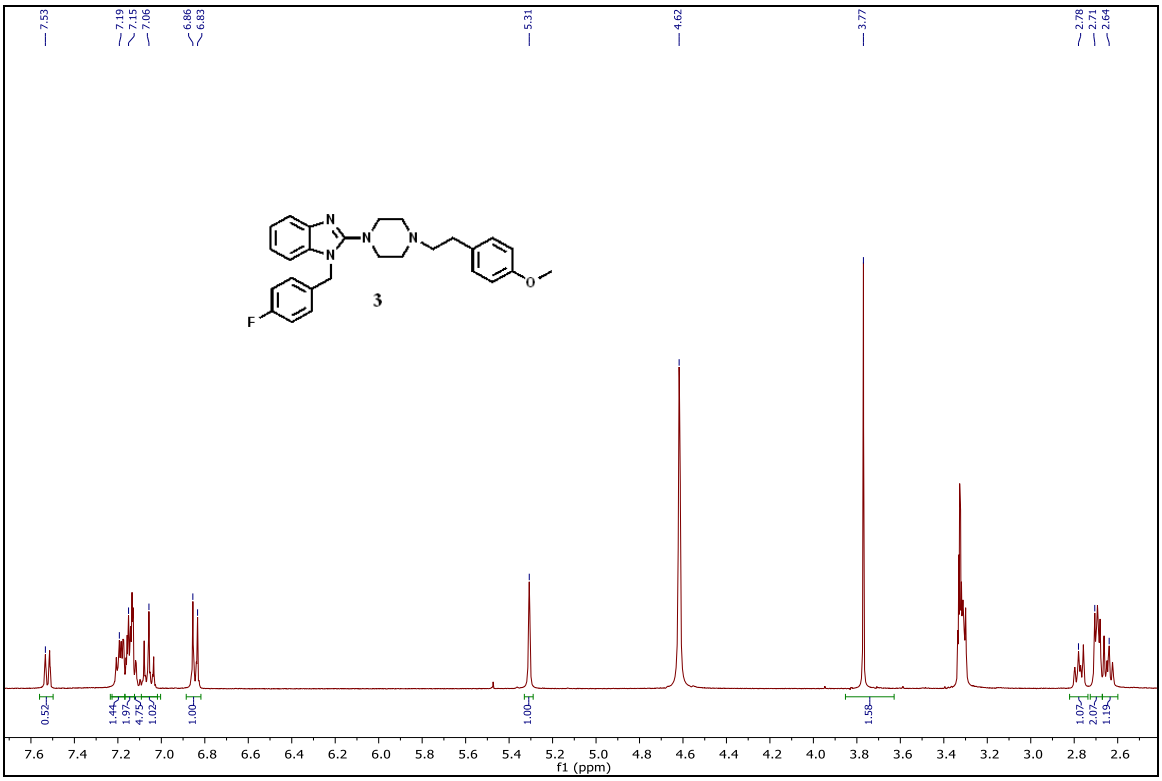

Figure S6: ^{1}H-NMR spectrum of **3** in CD_3OD at 400 MHz.

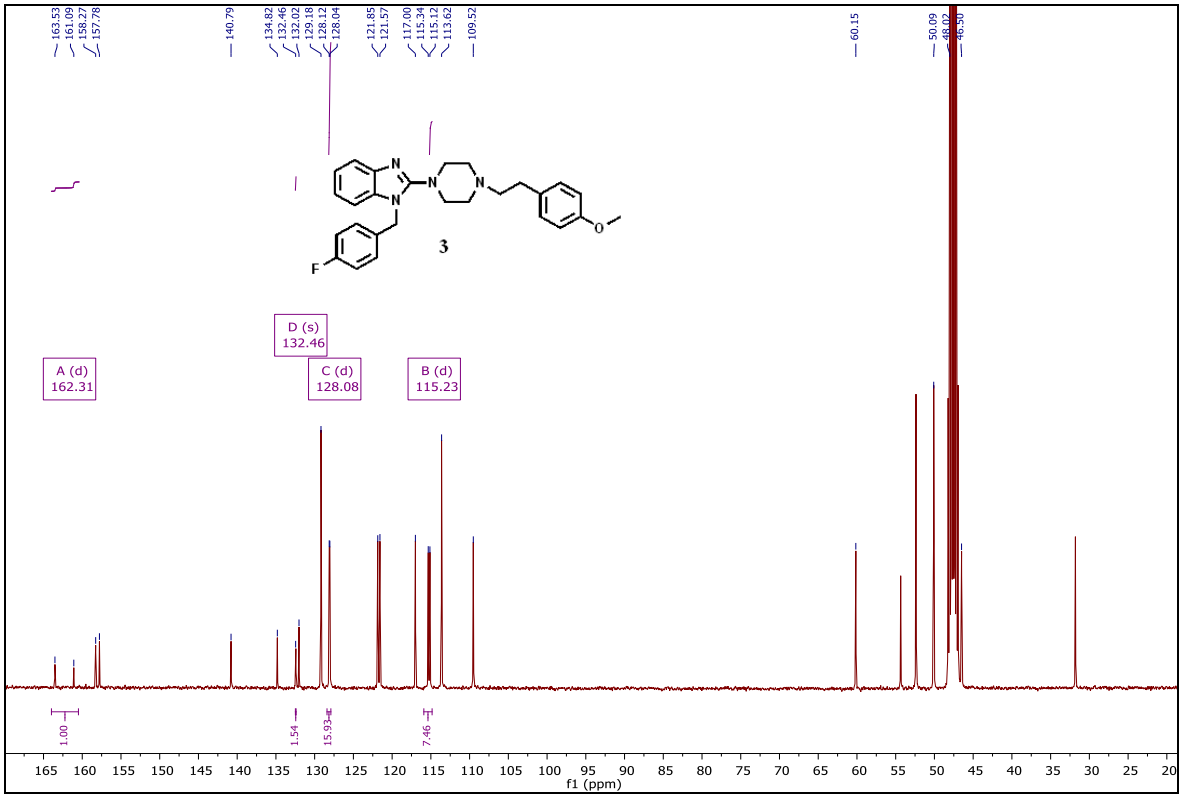

Figure S7: ^{13}C-NMR spectrum of **3** in CD_3OD at 101 MHz.

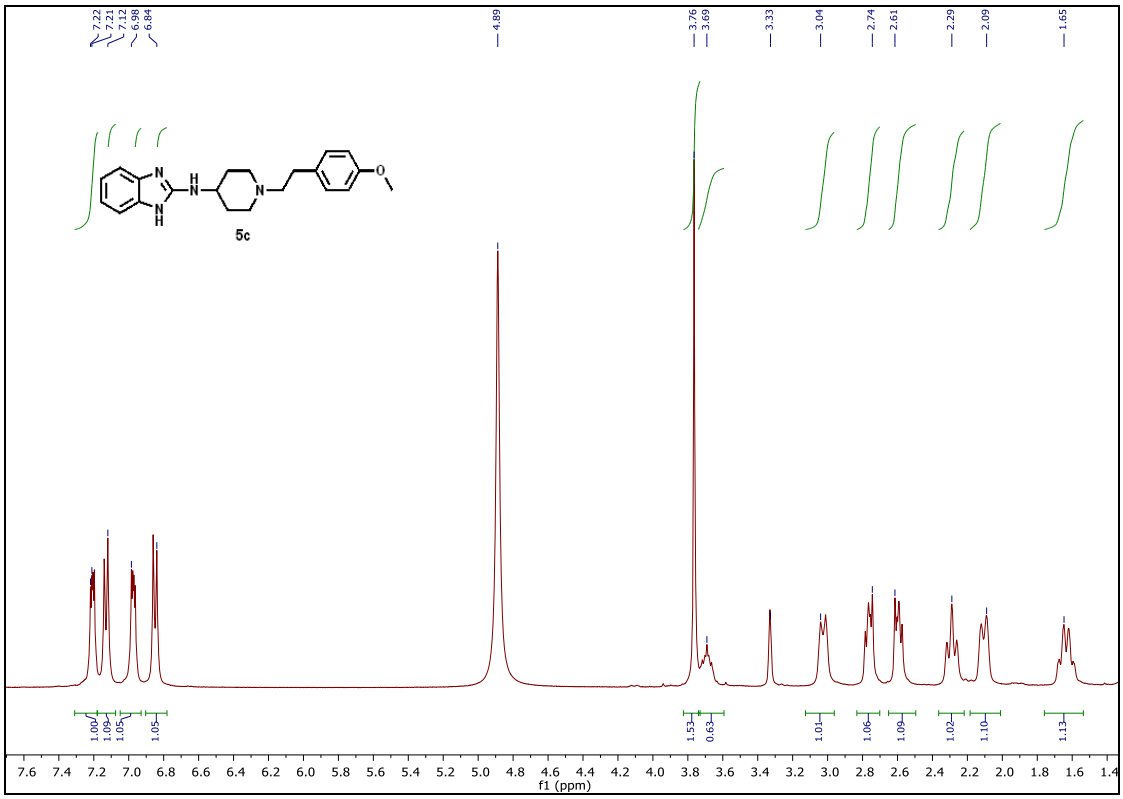

Figure S8: ^{1}H-NMR spectrum of **5c** in CD_3OD at 400 MHz.

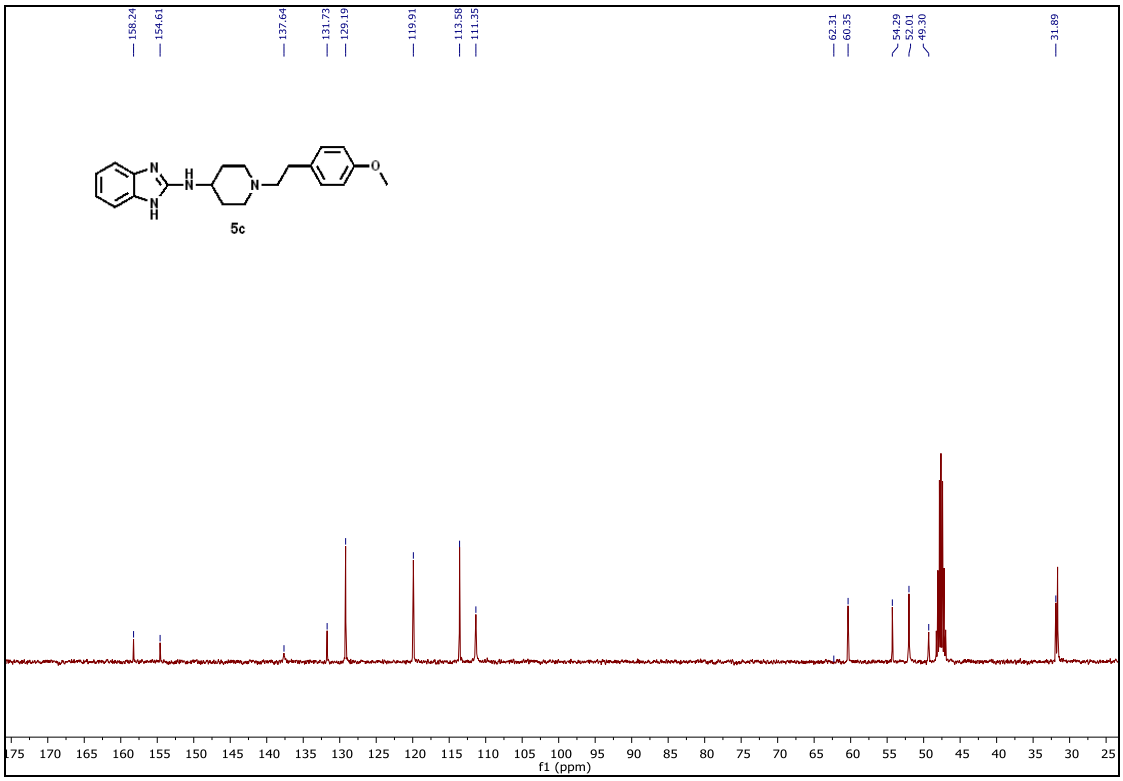

Figure S9: ^{13}C-NMR spectrum of **5c** in CD_3OD at 101 MHz.

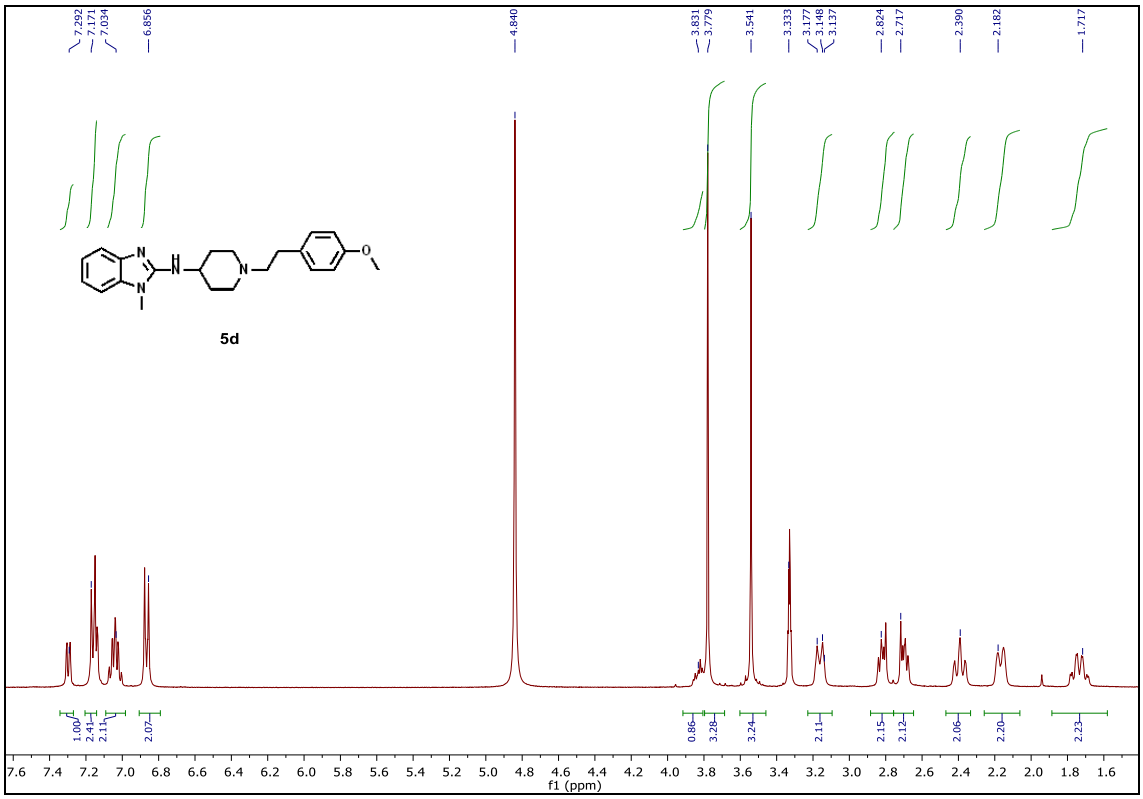

Figure S10: ^{1}H-NMR spectrum of **5d** in CD_3OD at 400 MHz.

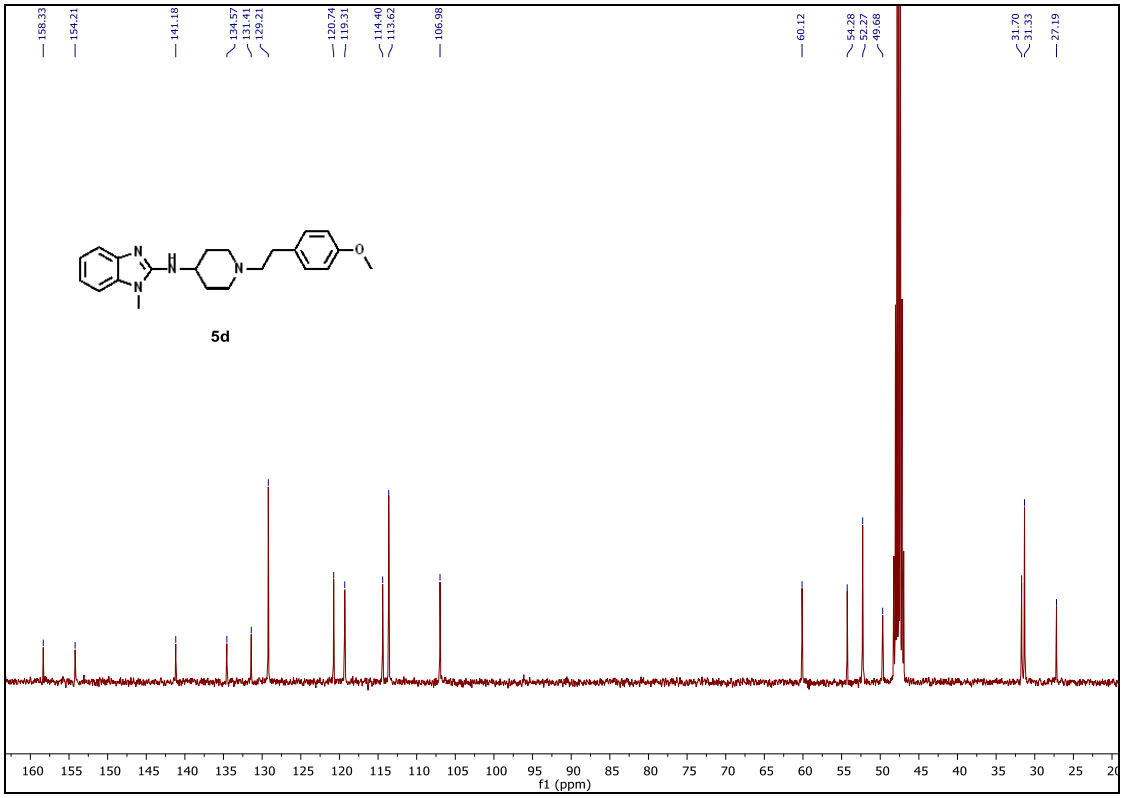

Figure S11: ^{13}C-NMR spectrum of **5d** in CD_3OD at 101 MHz.

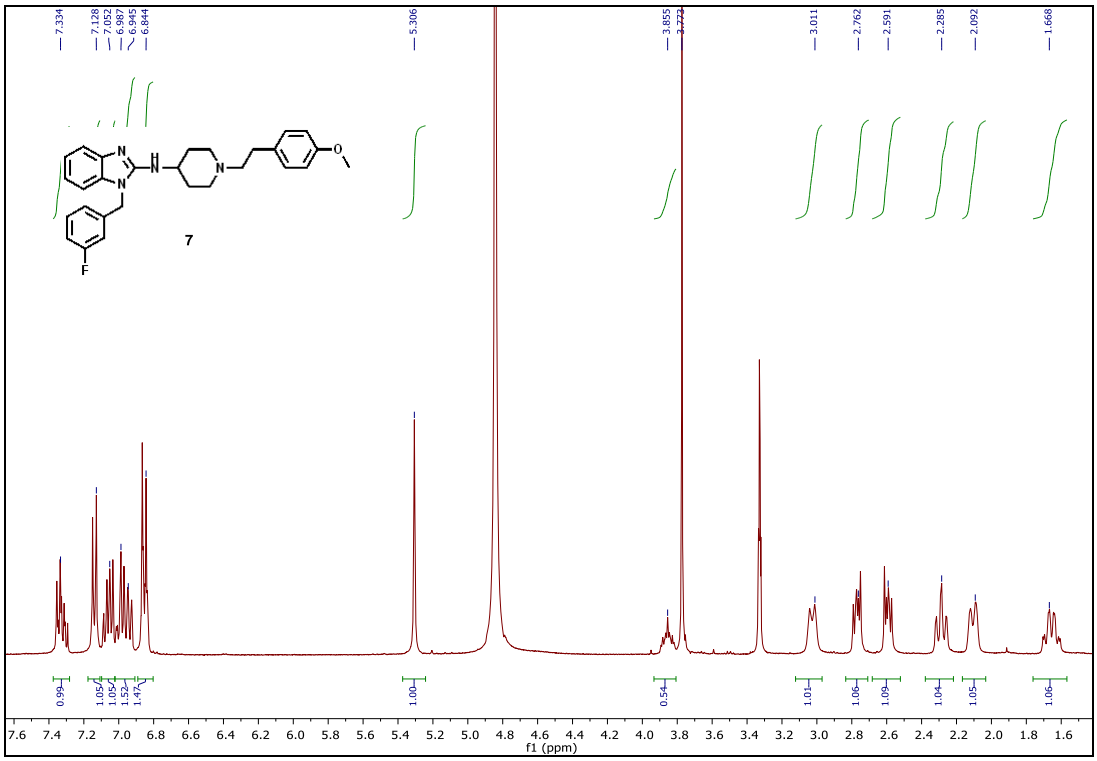

Figure S12: ^{1}H-NMR spectrum of **7** in CD_3OD at 400 MHz.

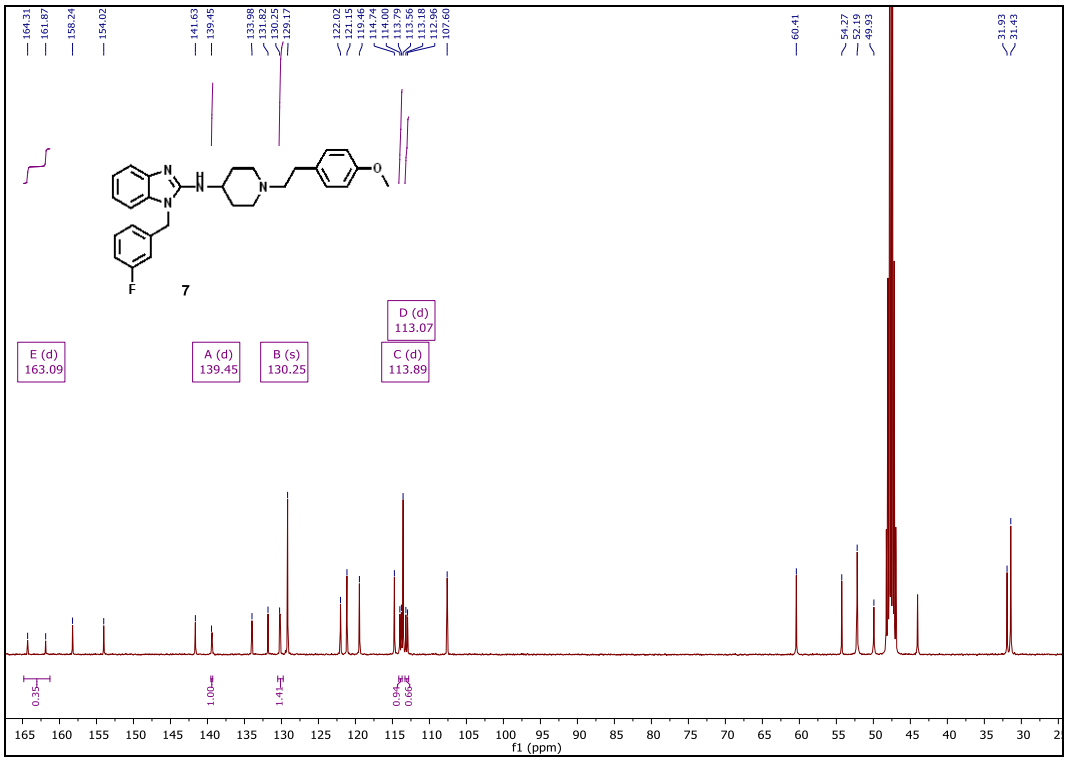

Figure S13: ^{13}C-NMR spectrum of **7** in CD_3OD at 101 MHz.

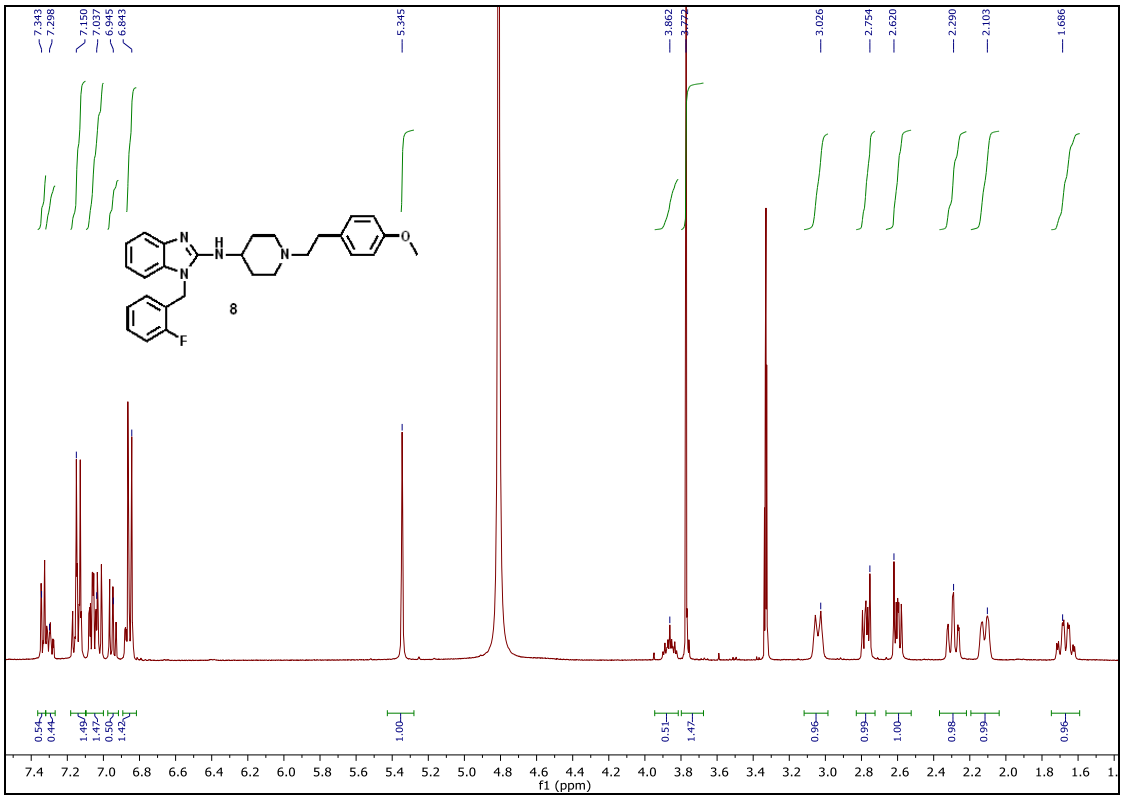

Figure S14: ^{1}H-NMR spectrum of **8** in CD_3OD at 400 MHz.

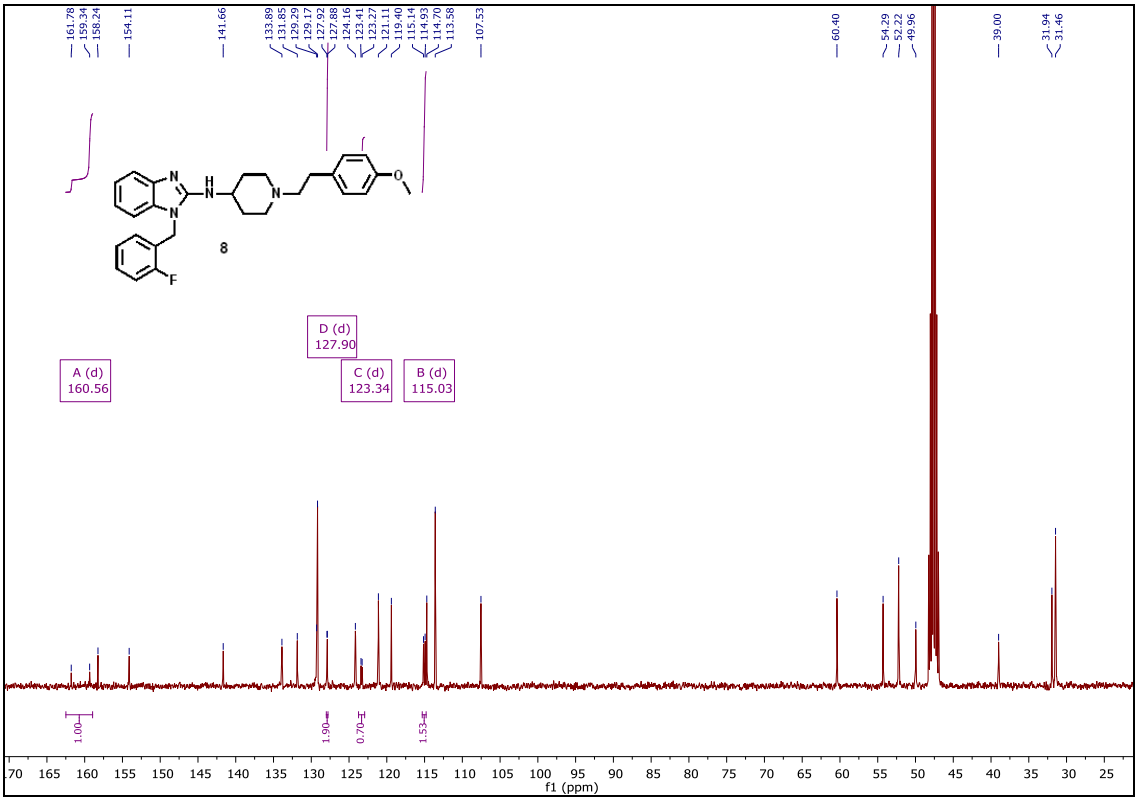

Figure S15: ^{13}C-NMR spectrum of **8** in CD_3OD at 101 MHz.

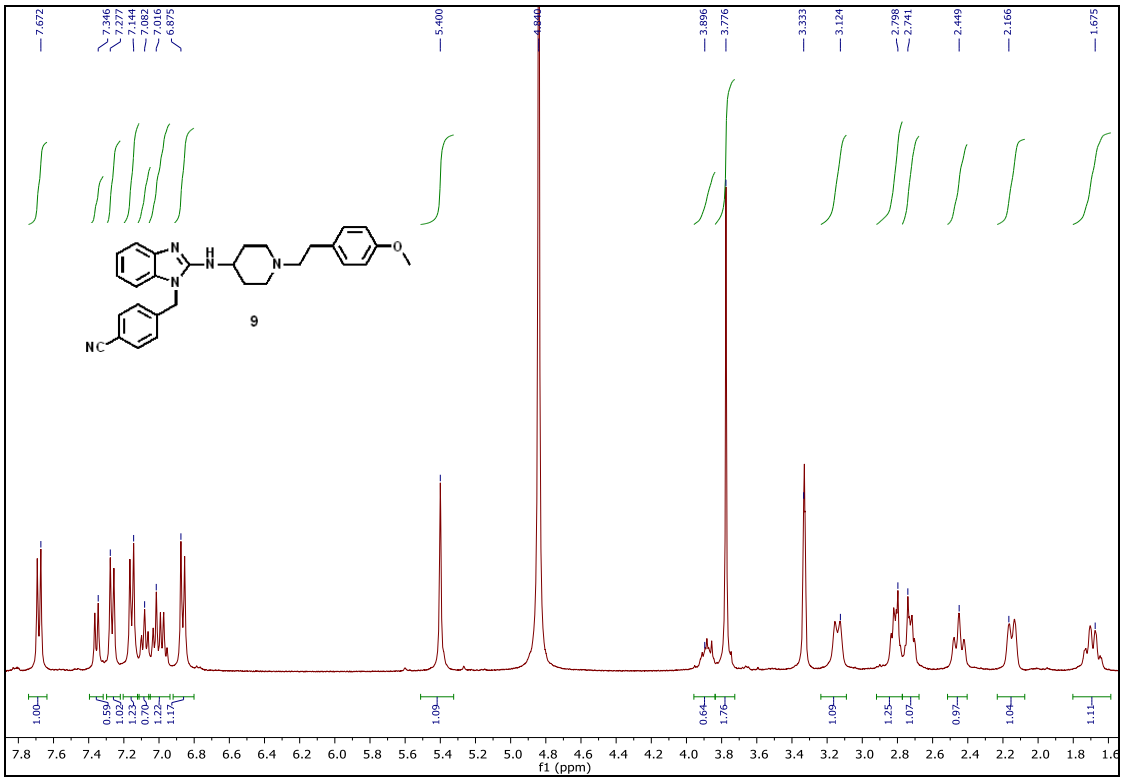

Figure S16: ^{1}H-NMR spectrum of **9** in CD_3OD at 400 MHz.

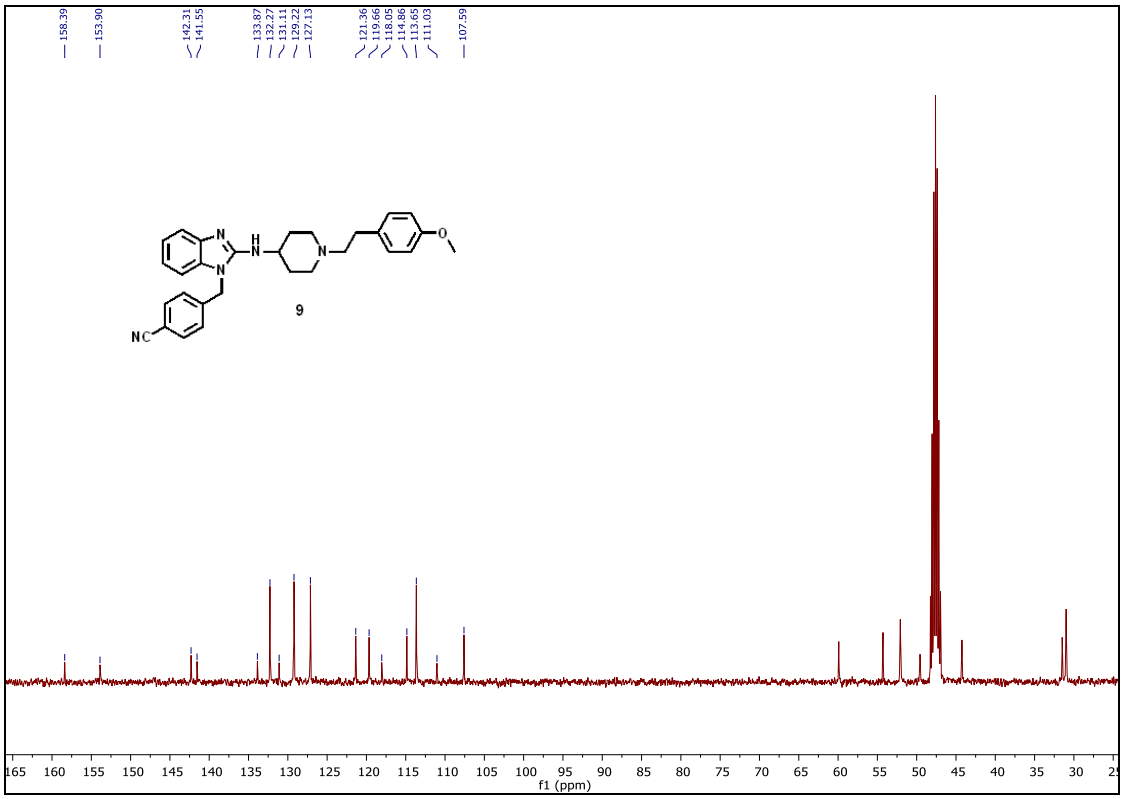

Figure S17: ^{13}C-NMR spectrum of **9** in CD_3OD at 101 MHz.

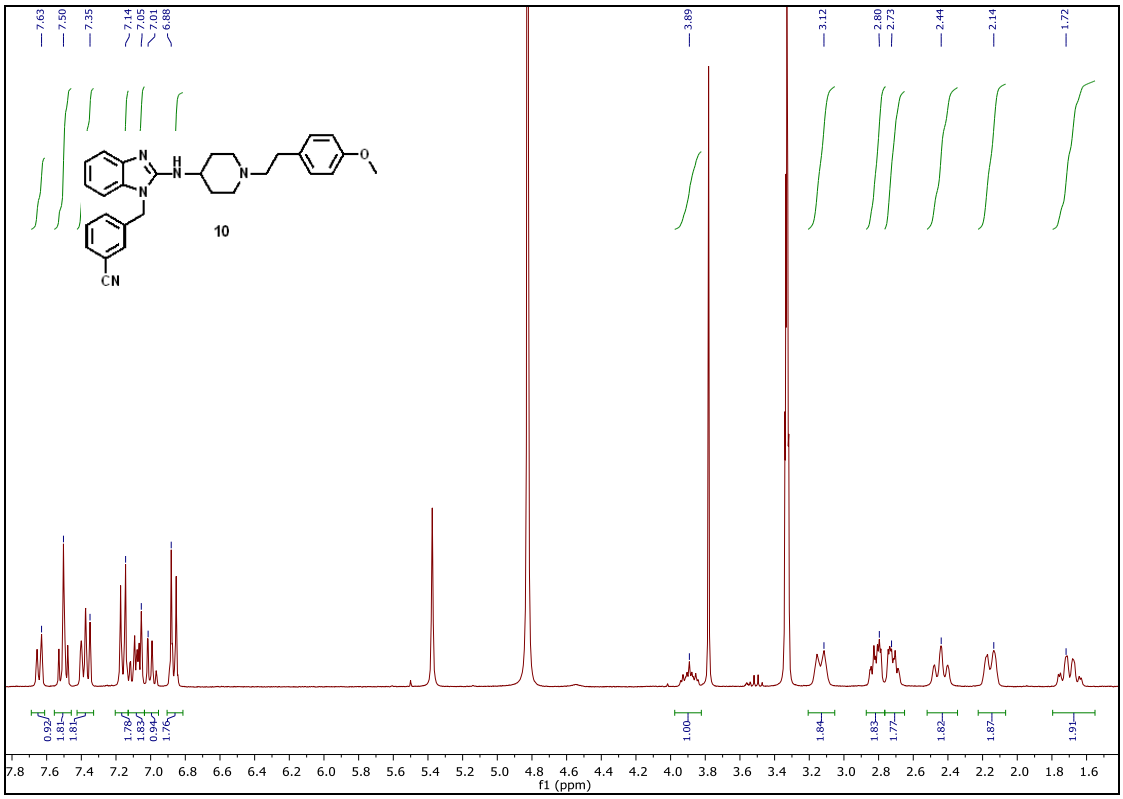

Figure S18: ^{1}H-NMR spectrum of **10** in CD_3OD at 300 MHz.

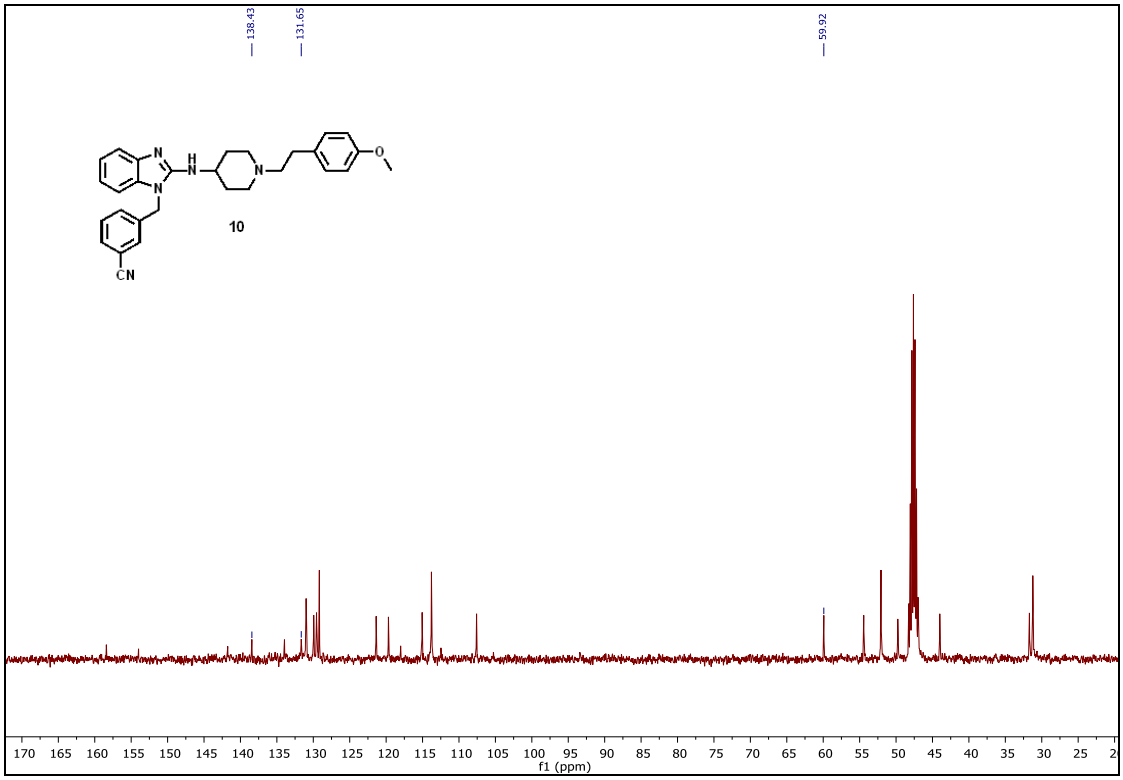

Figure S19: ^{13}C-NMR spectrum of **10** in CD_3OD at 101 MHz.

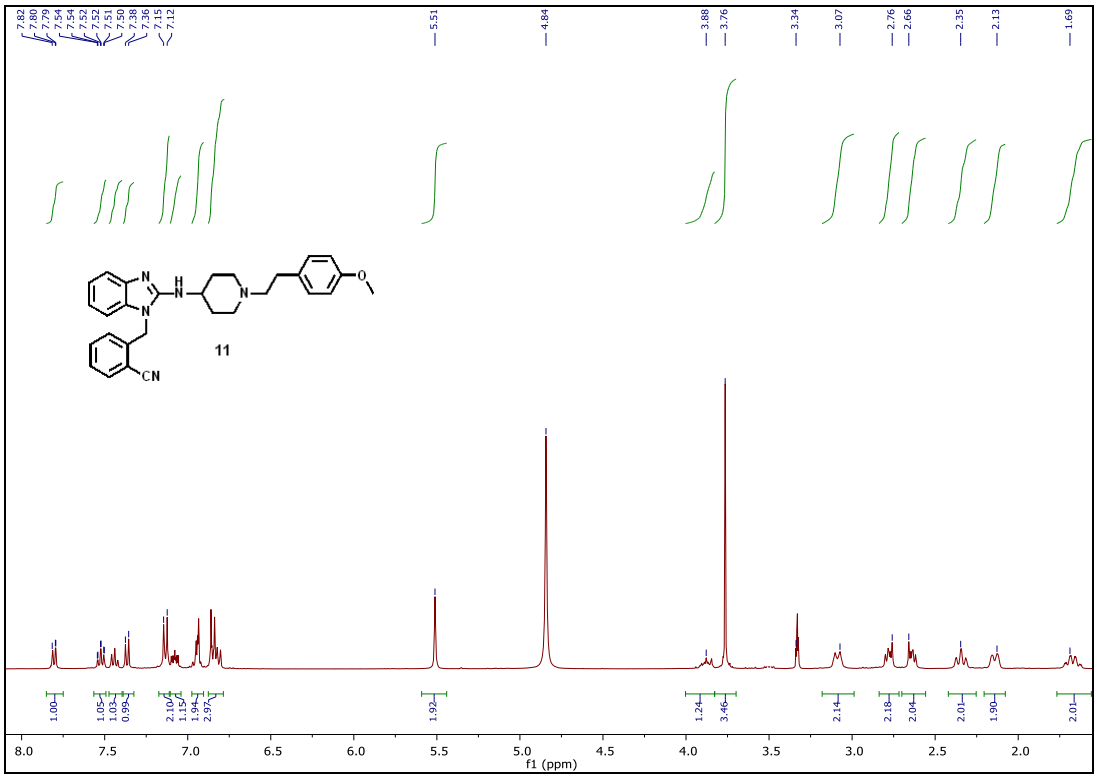

Figure S20: ^{1}H-NMR spectrum of **11** in CD_3OD at 400 MHz.

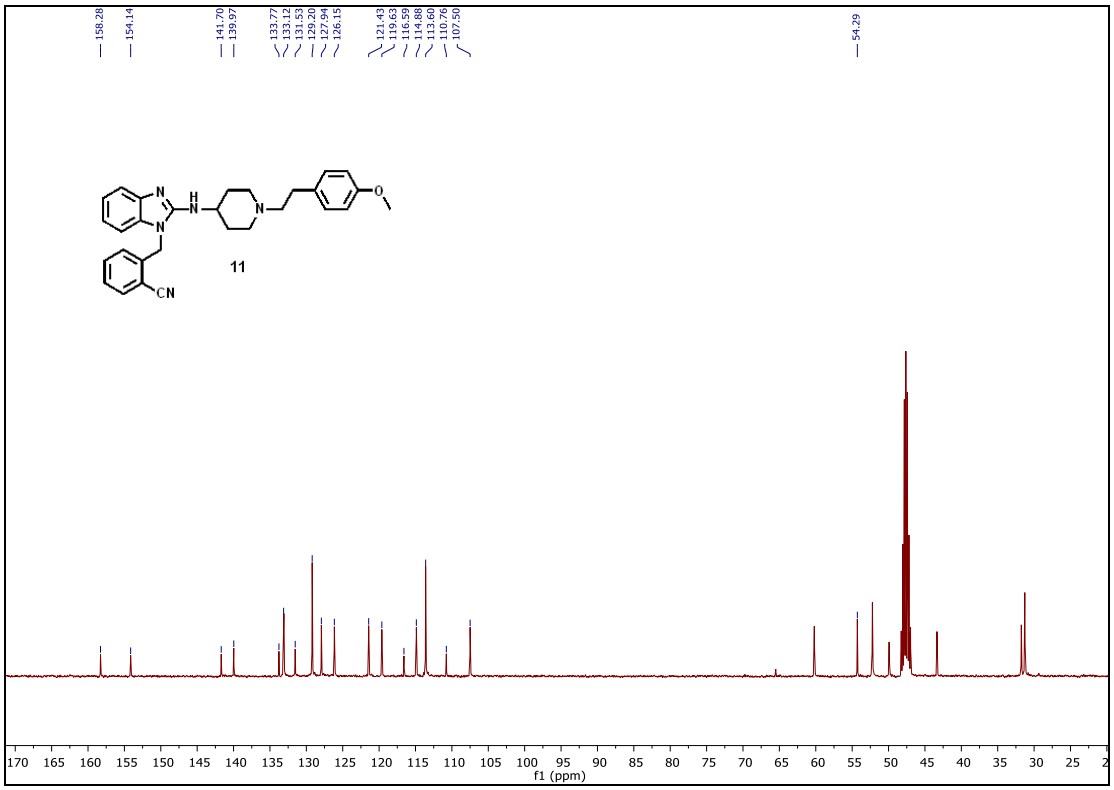

Figure S21: ^{13}C-NMR spectrum of **11** in CD_3OD at 101 MHz.

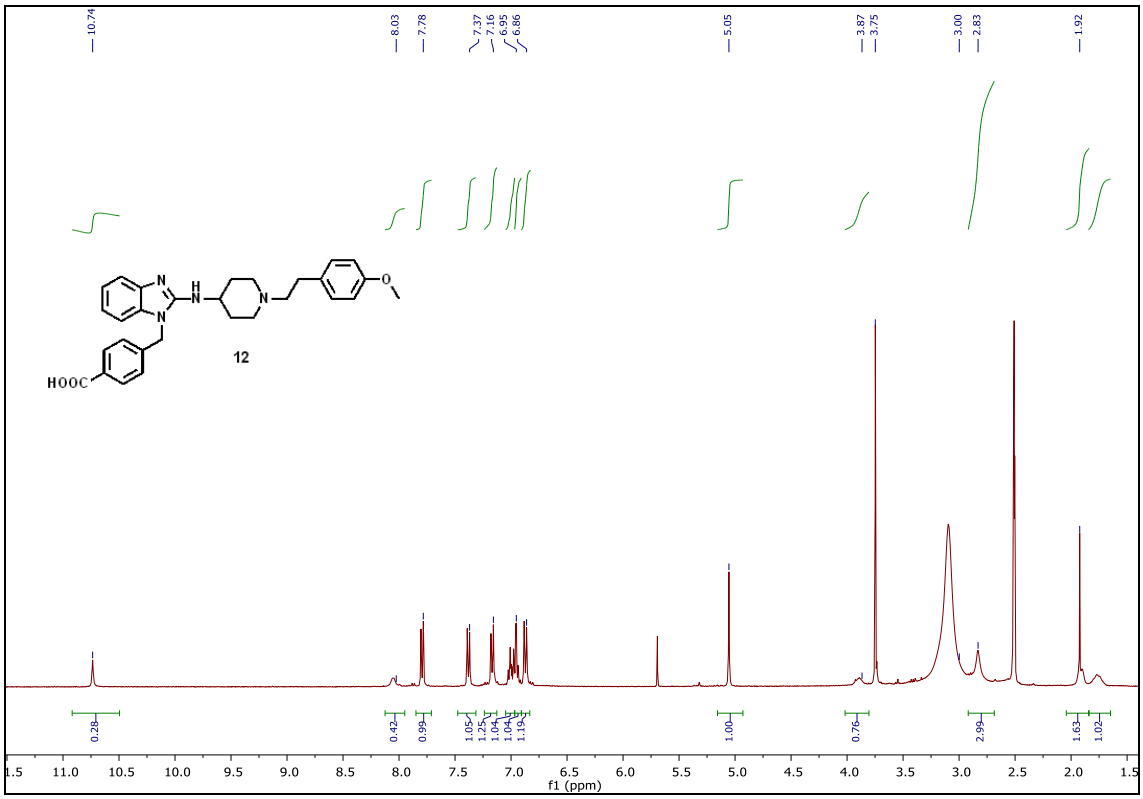

Figure S22: ^{1}H-NMR spectrum of **12** in DMSO @ 80 ºC at 400 MHz.

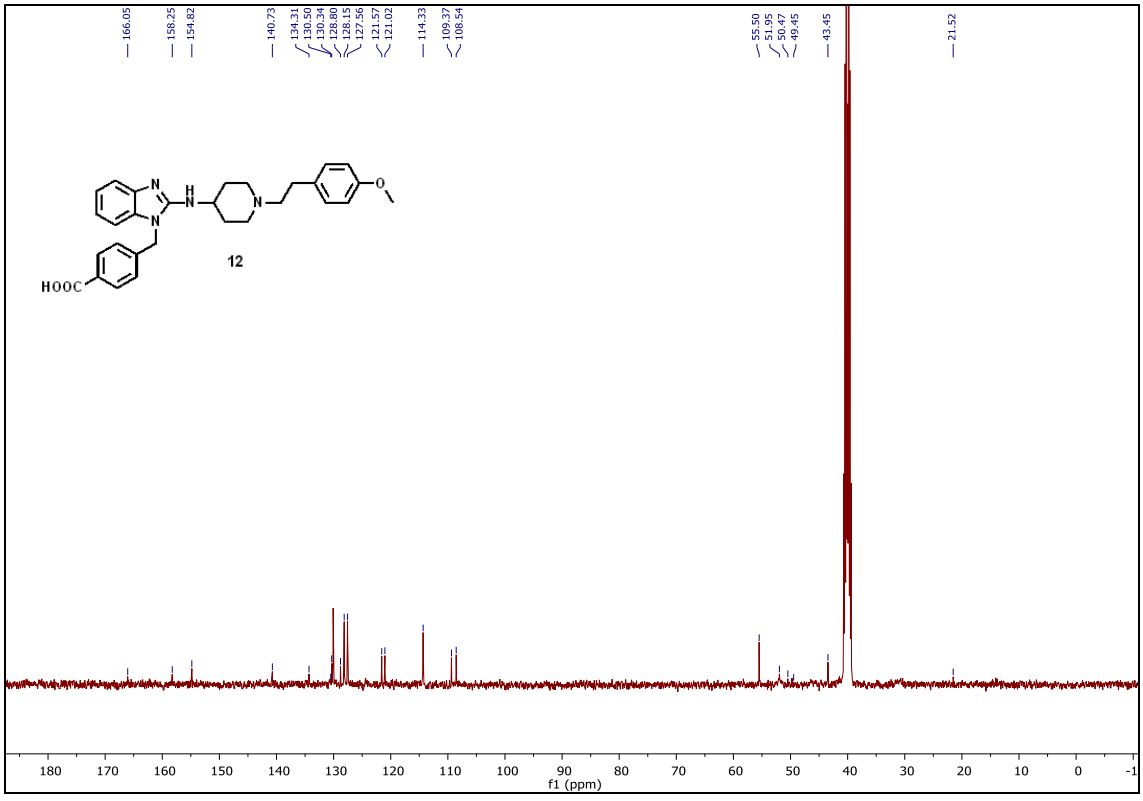

Figure S23: ^{13}C-NMR spectrum of **12** in DMSO at 101 MHz.

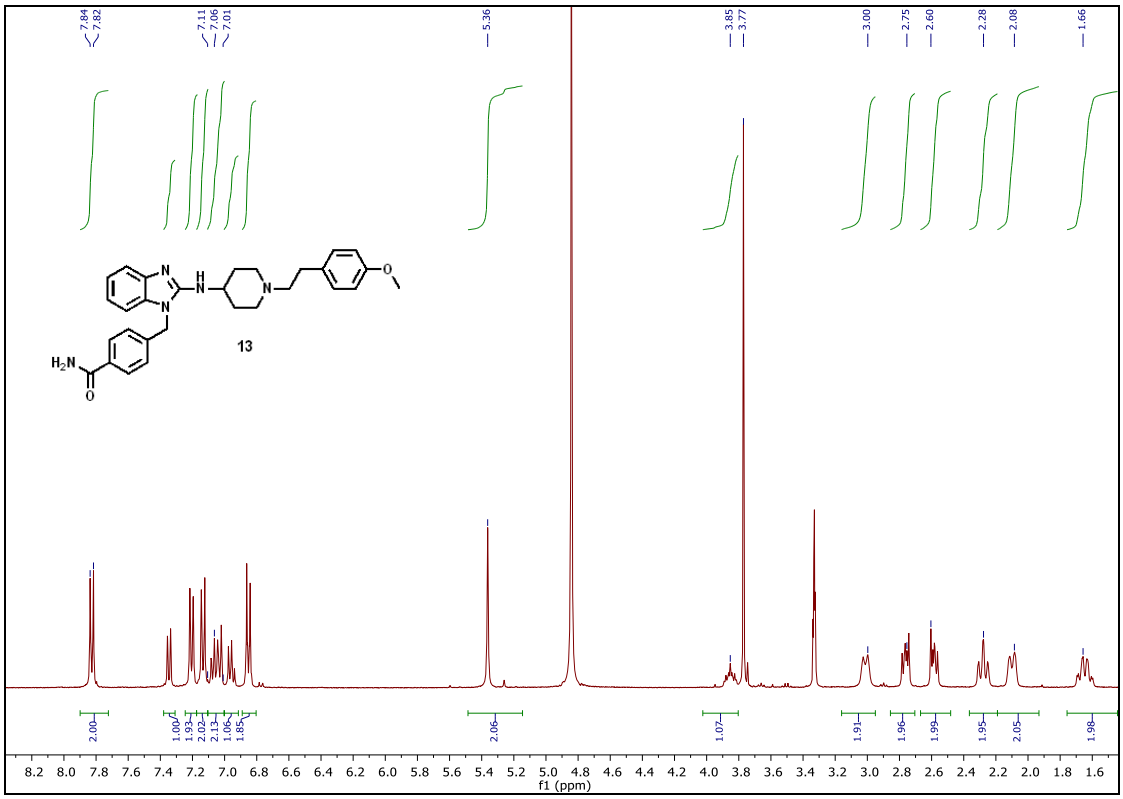

Figure S24: ^{1}H-NMR spectrum of **13** in CD_3OD at 400 MHz.

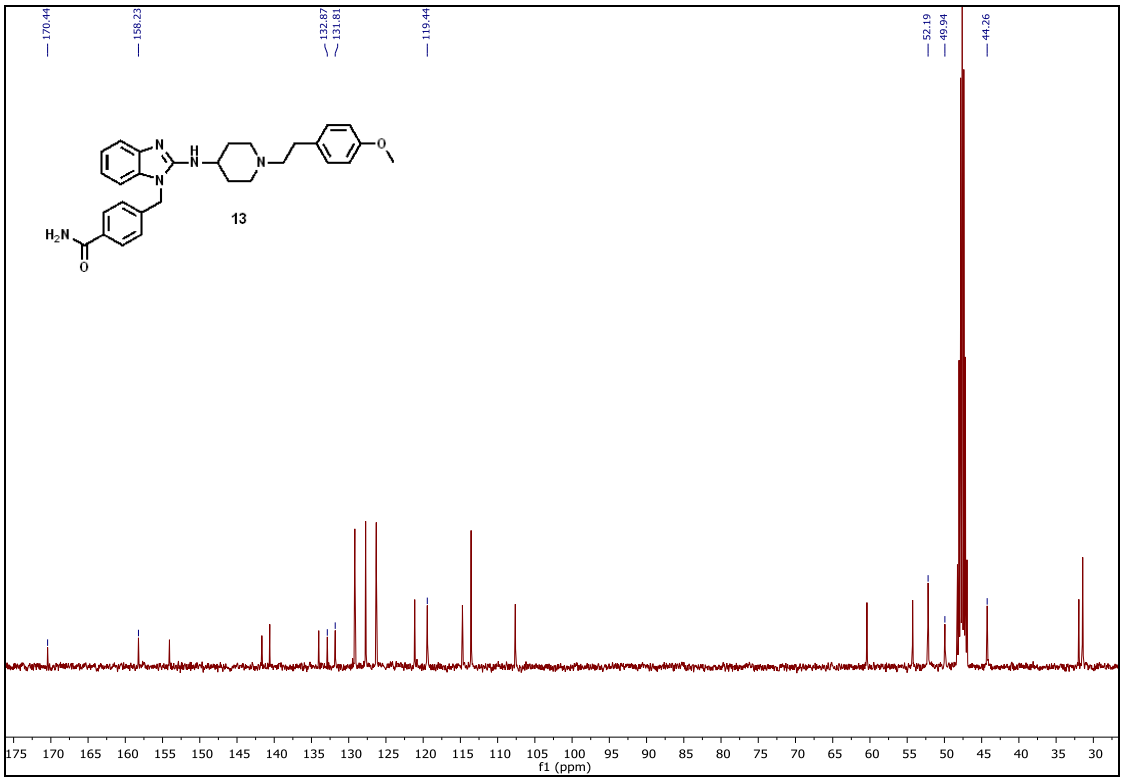

Figure S25: ^{13}C-NMR spectrum of **13** in CD_3OD at 101 MHz.

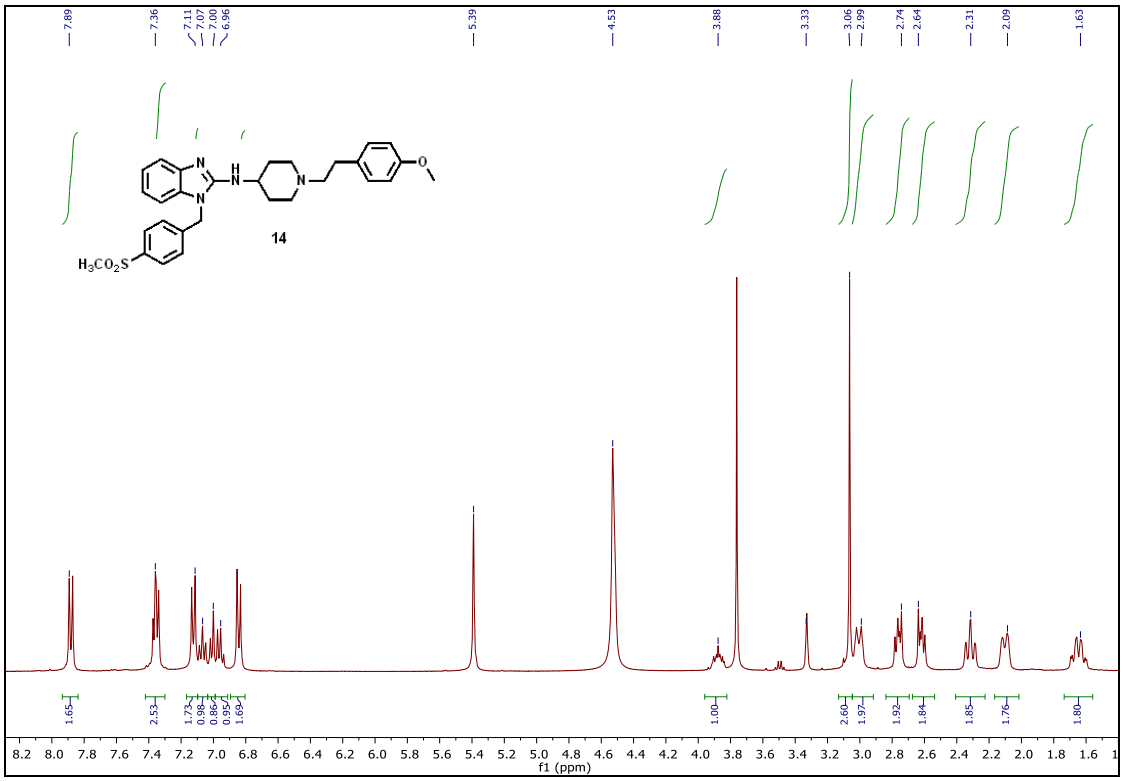

Figure S26: ^{1}H-NMR spectrum of **14** in CD_3OD at 400 MHz.

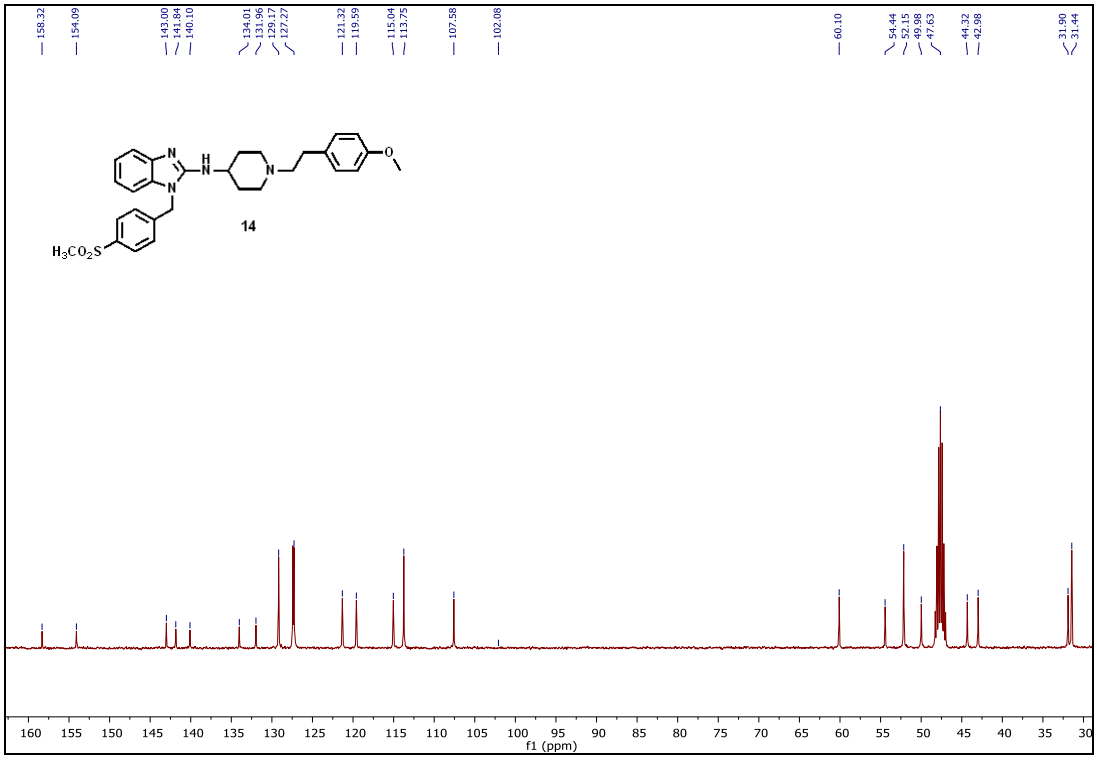

Figure S27: ^{13}C-NMR spectrum of **14** in CD_3OD at 101 MHz.

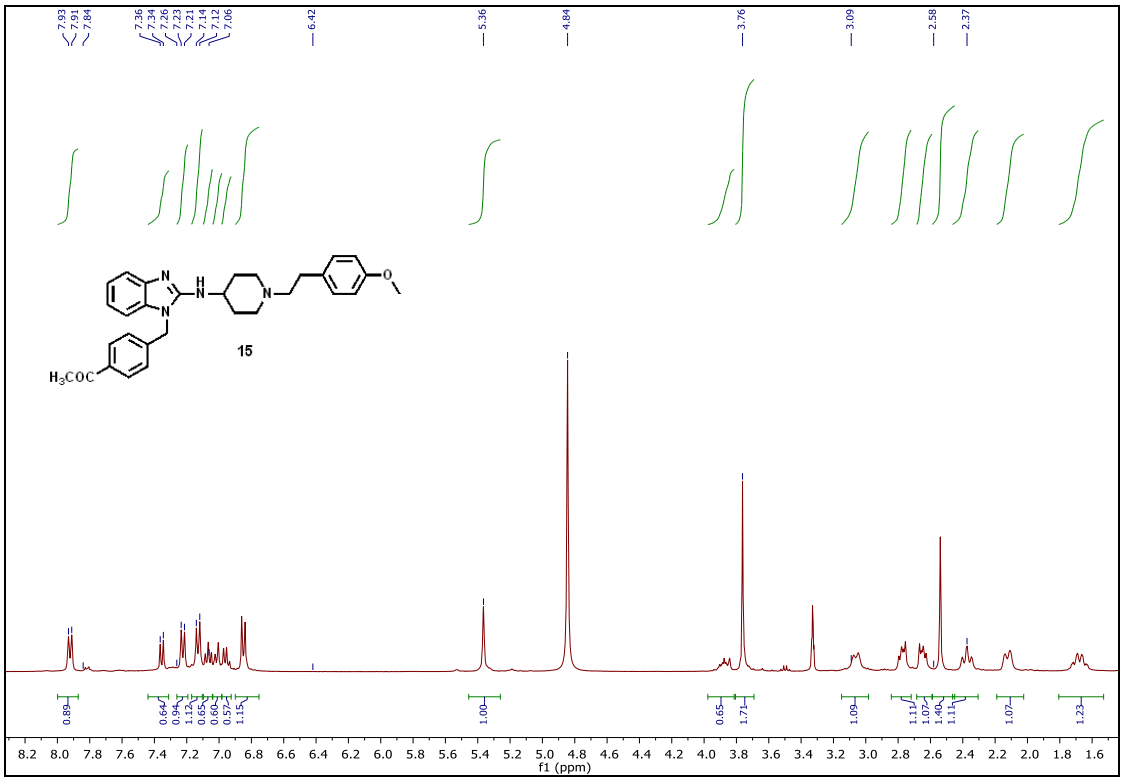

Figure S28: ^{1}H-NMR spectrum of **15** in CD_3OD at 400 MHz.

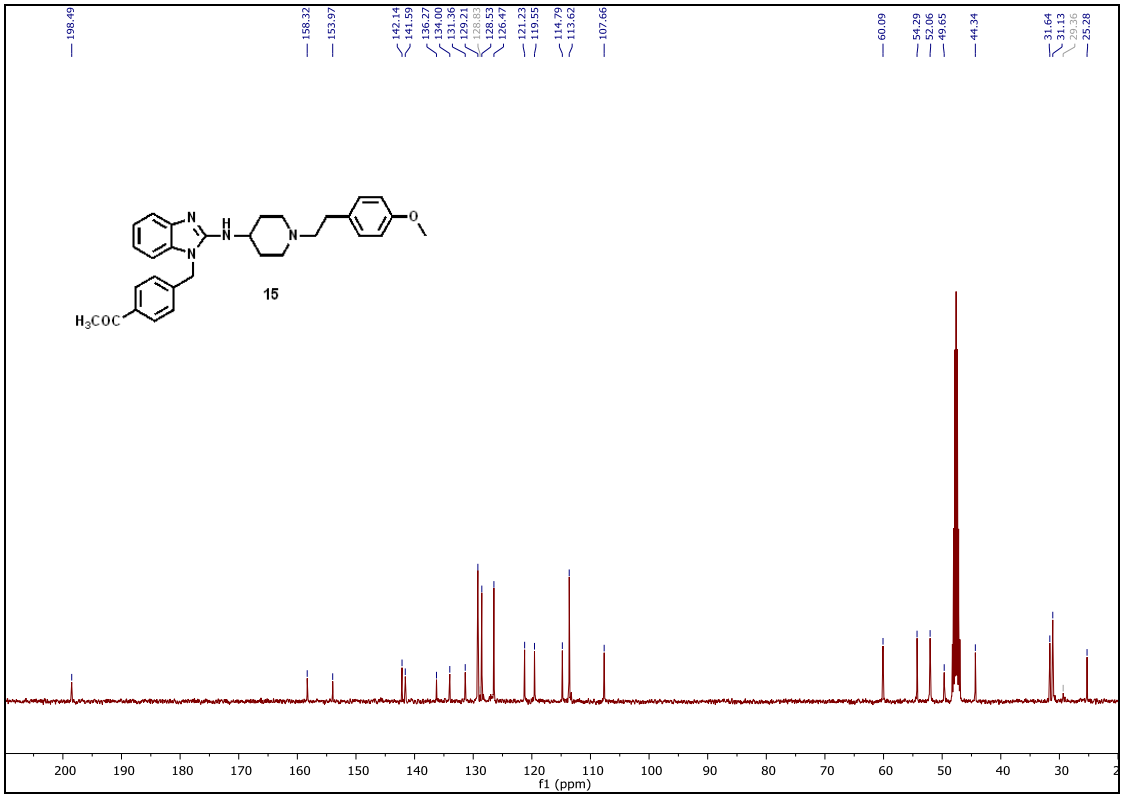

Figure S29: ^{13}C-NMR spectrum of **15** in CD_3OD at 101 MHz.

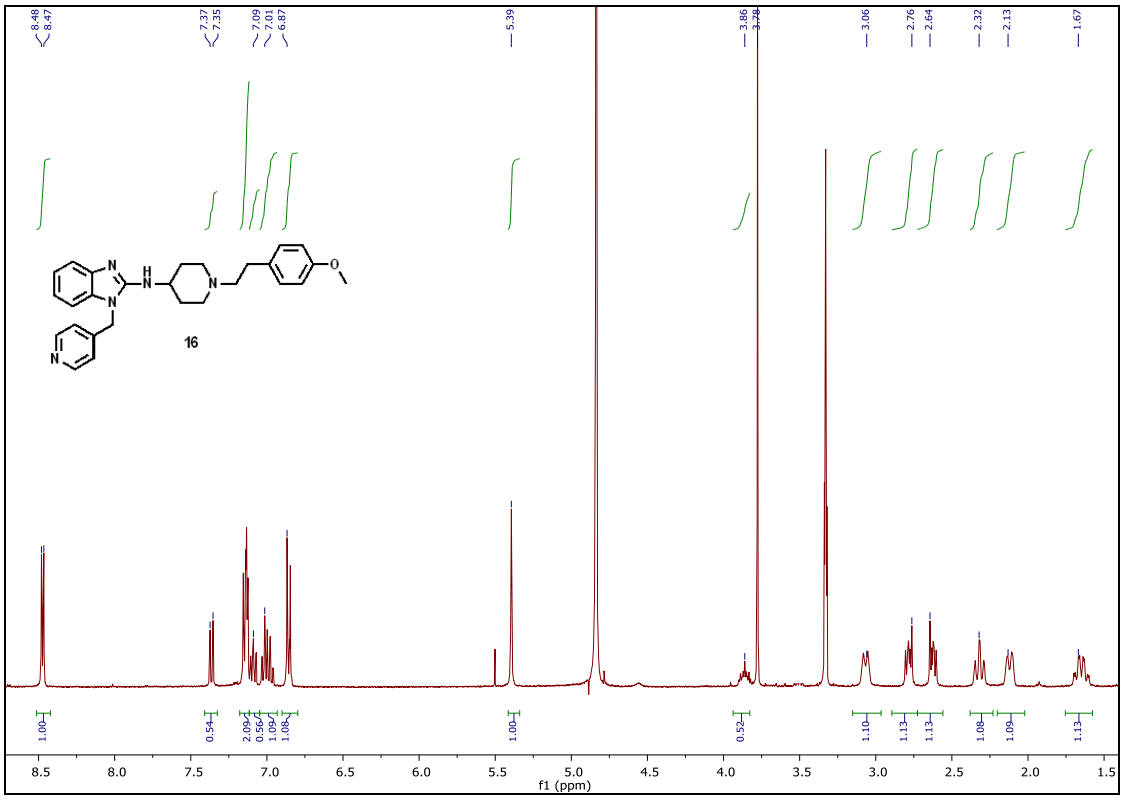

Figure S30: ^{1}H-NMR spectrum of **16** in CD_3OD at 400 MHz.

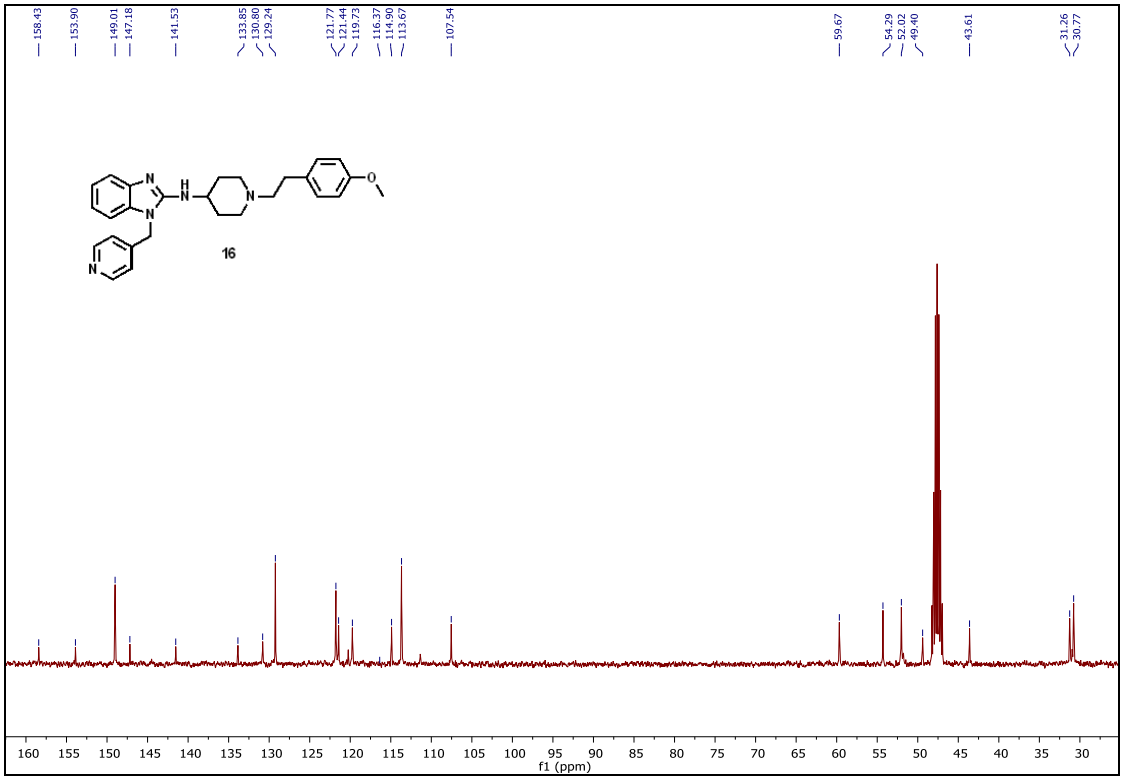

Figure S31: ^{13}C-NMR spectrum of **16** in CD_3OD at 101 MHz.

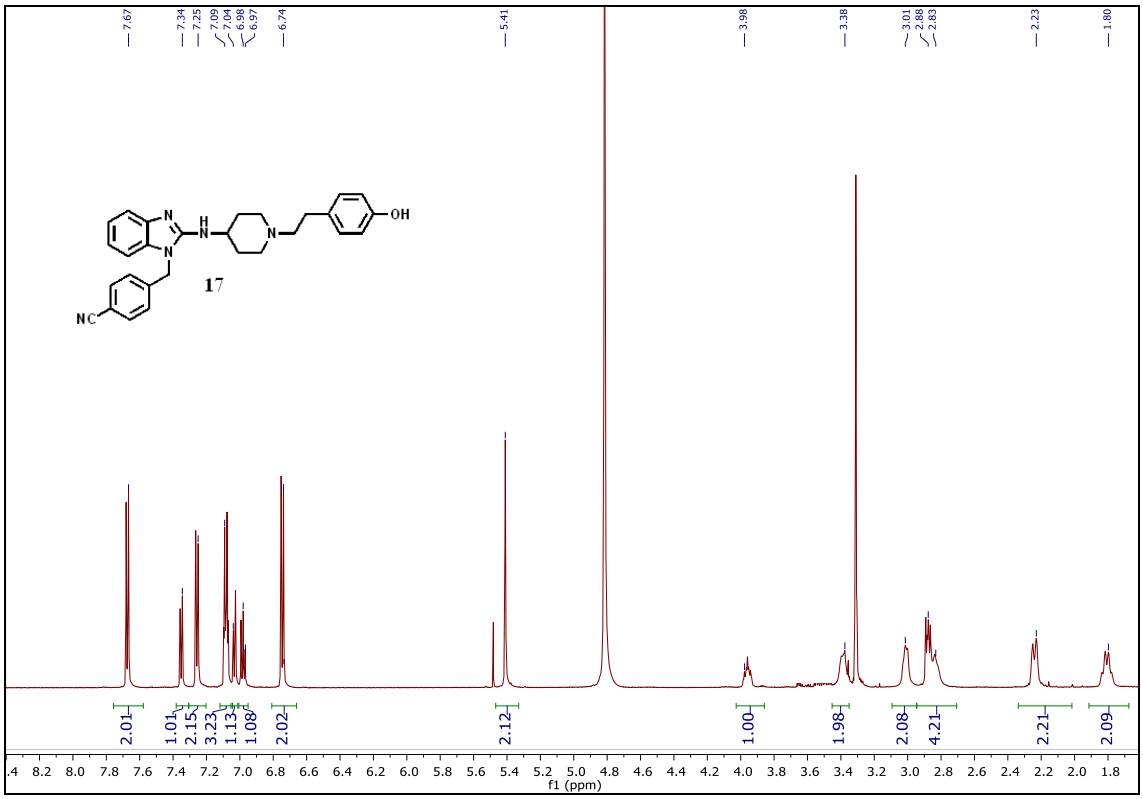

Figure S32: ^{1}H-NMR spectrum of **17** in CD_3OD at 600 MHz.

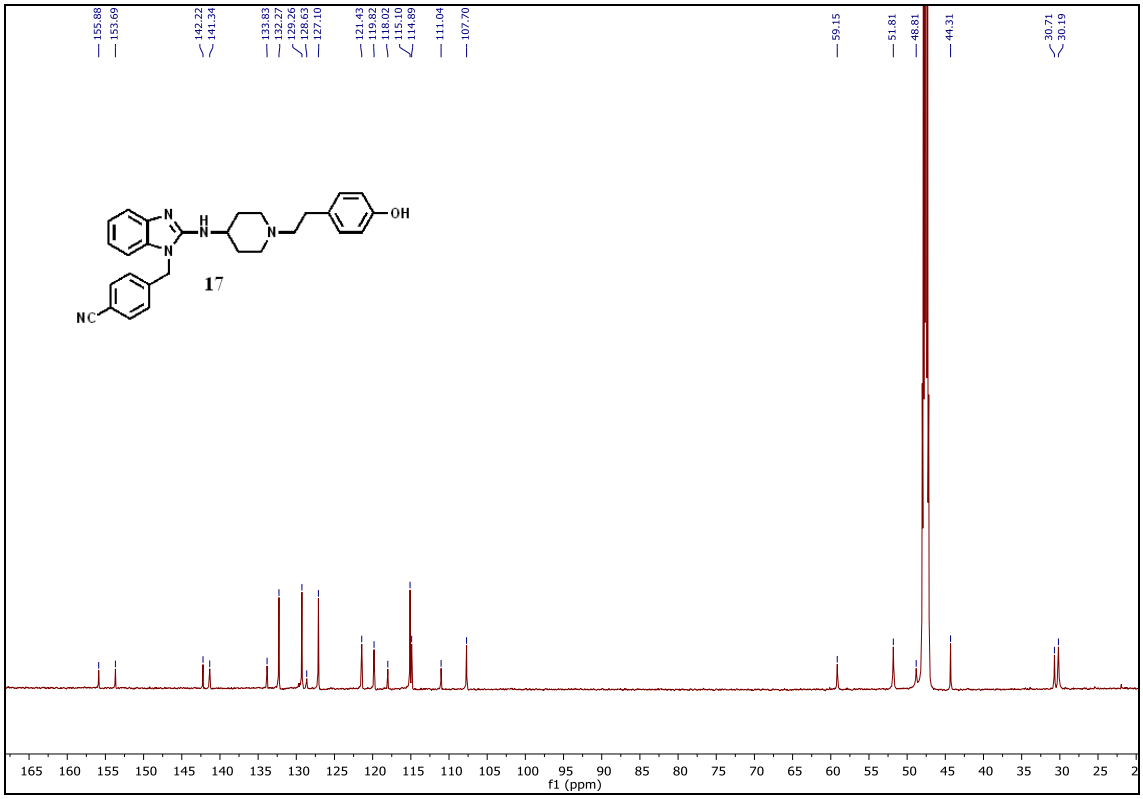

Figure S33: ^{13}C-NMR spectrum of **17** in CD_3OD at 151 MHz.

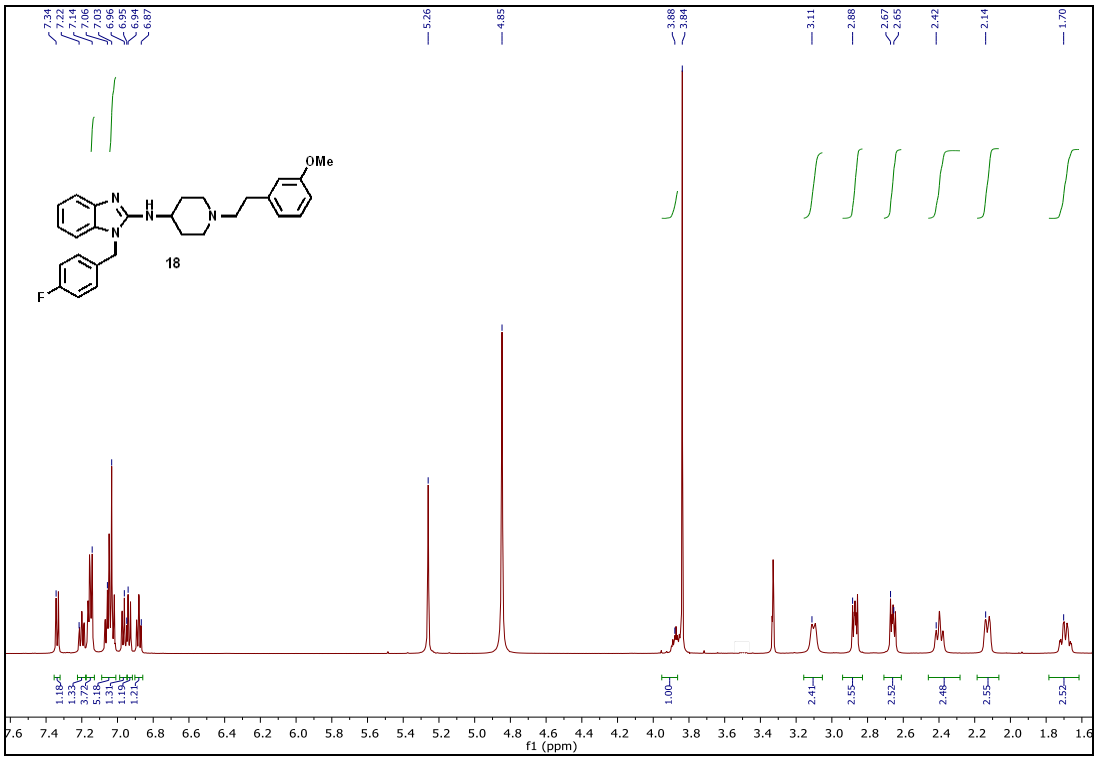

Figure S34: ^{1}H-NMR spectrum of **18** in CD_3OD at 600 MHz.

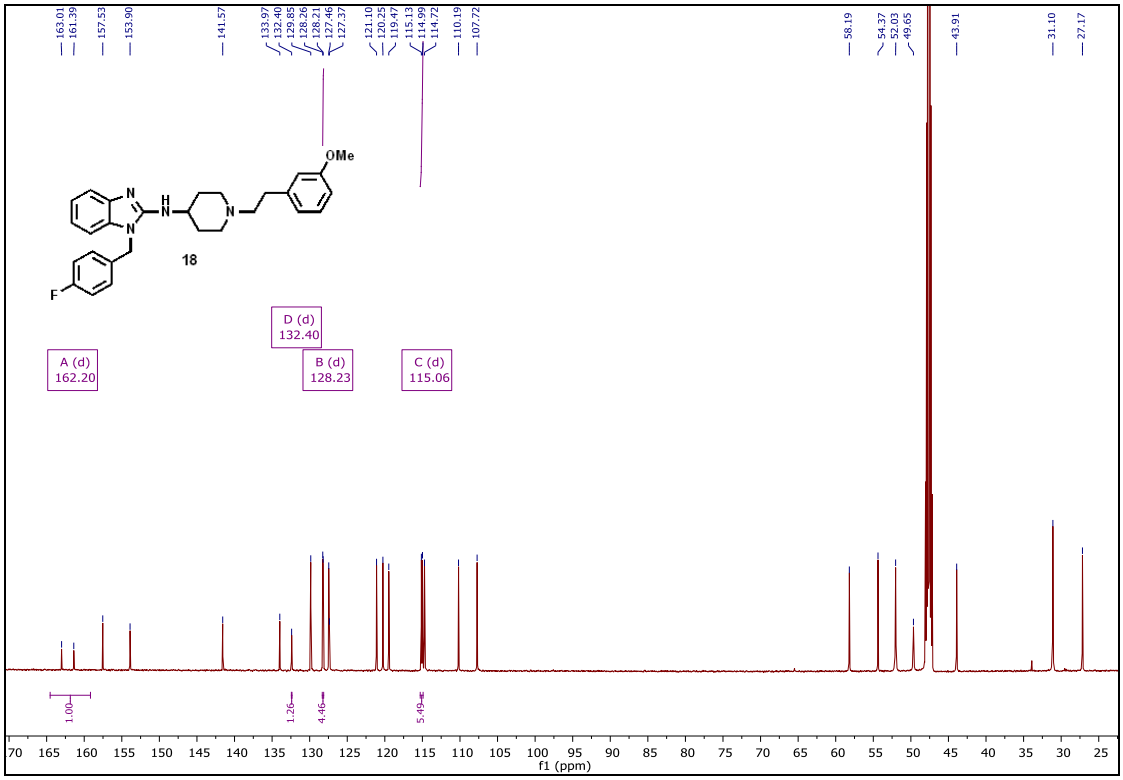

Figure S35: ^{13}C-NMR spectrum of **18** in CD_3OD at 151 MHz.

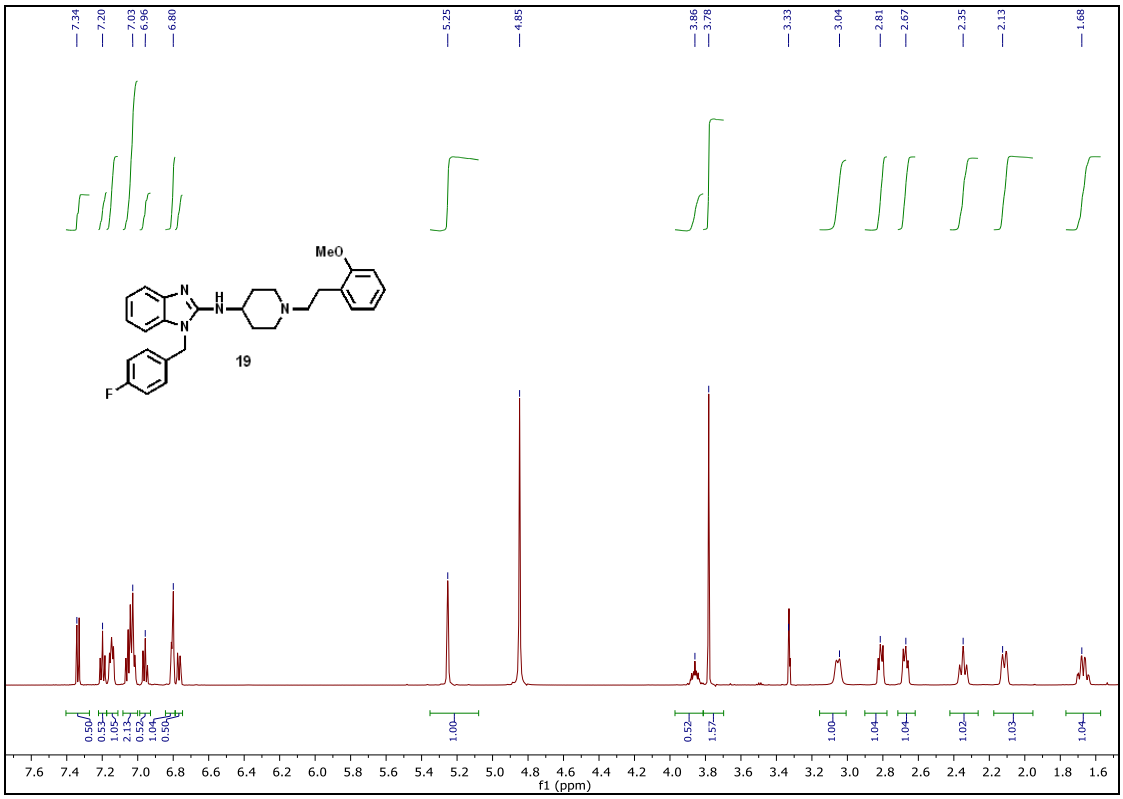

Figure S36: ^{1}H-NMR spectrum of **19** in CD_3OD at 600 MHz.

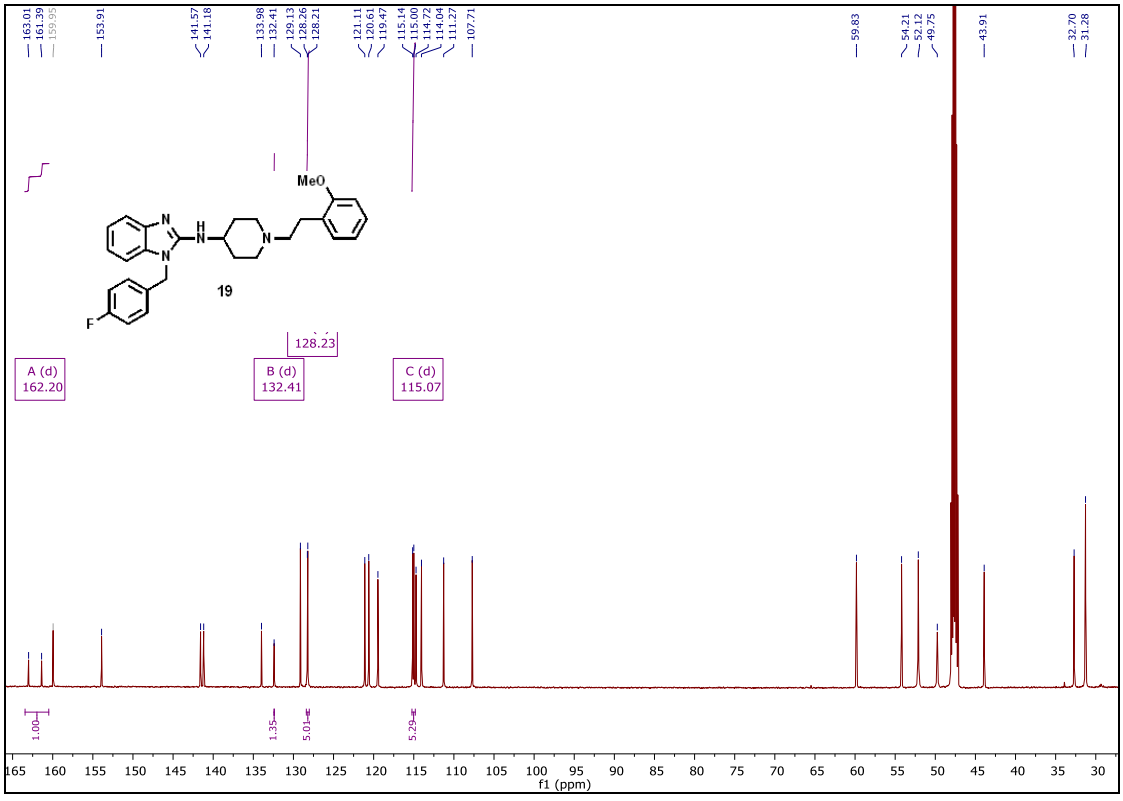

Figure S37: ^{13}C-NMR spectrum of **19** in CD_3OD at 151 MHz.

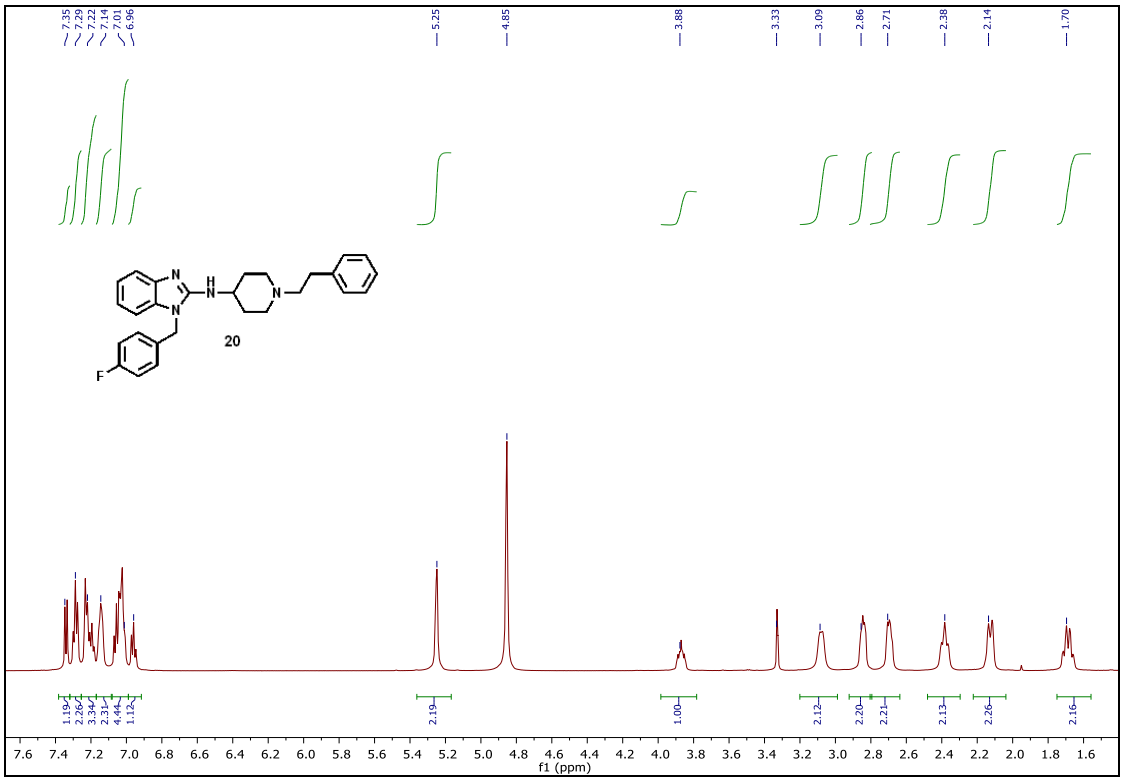

Figure S38: ^{1}H-NMR spectrum of **20** in CD_3OD at 600 MHz.

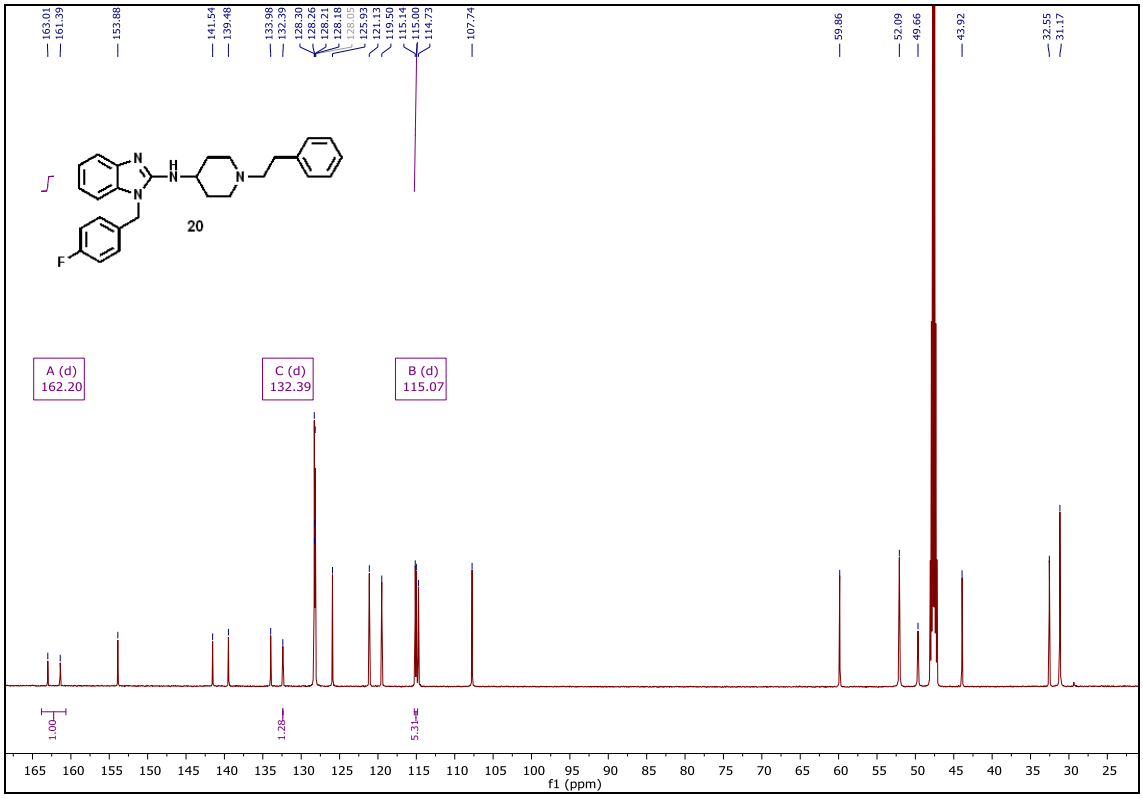

Figure S39: ^{13}C-NMR spectrum of **20** in CD_3OD at 151 MHz.